

WATER RESOURCES DEVELOPMENT PROJECT

TRUMBULL LAKE

PEQUONNOCK RIVER BASIN, CONNECTICUT

DESIGN MEMORANDUM NO. 4a

CONCRETE MATERIALS SUPPLEMENT



DEPARTMENT OF THE ARMY
NEW ENGLAND DIVISION, CORPS OF ENGINEERS
WALTHAM, MASS.

APRIL 1972

20



DEPARTMENT OF THE ARMY
NEW ENGLAND DIVISION, CORPS OF ENGINEERS
424 TRAPELO ROAD
WALTHAM, MASSACHUSETTS 02154

IN REPLY REFER TO:

NEDED-E

27 April 1972

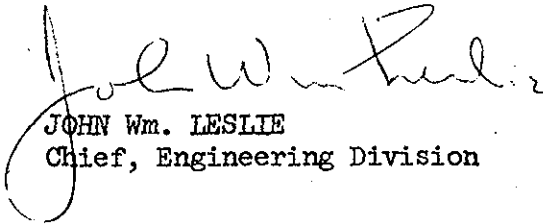
SUBJECT: Trumbull Lake, Pequonnock River Basin, Trumbull, Connecticut
Supplement No. 4a to Design Memorandum No. 4, Concrete
Materials

HQDA (DAEN-CWE-C)
WASH DC 20314

1. There is submitted for review and approval, Supplement No. 4a to the Design Memorandum No. 4, Concrete Materials, for the Trumbull Lake Project.
2. As requested in your 1st Indorsement dated 27 April 71, this report supplements Design Memorandum No. 4, and extends the temperature study utilizing data developed at the Waterways Experiment Station, Vicksburg, Mississippi.
3. From this data, a maximum concrete placing temperature of 50°F is selected. Also the use of insulation with a value of 0.25 -U will be required to reduce cracking potential.

FOR THE DIVISION ENGINEER:

Incl (10 cys)
as


JOHN Wm. LESLIE
Chief, Engineering Division

WATER RESOURCES DEVELOPMENT PROJECT

TRUMBULL LAKE

PEQUONNOCK RIVER

PEQUONNOCK RIVER BASIN

CONNECTICUT

Design Memorandum Index

<u>No.</u>	<u>Title</u>	<u>Scheduled Submission Date</u>	<u>Date Submitted</u>	<u>Date Approved</u>
1	Hydrology	-	31 Mar 69	5 Jun 69
2	General Design	-	22 Jul 71	8 Nov 71
3	Land Requirement Plan - Public Use	-	9 Apr 70	30 Jun 70
4	Concrete Materials	-	24 Nov 70	4 Aug 71
4a	Concrete Materials - Supplement	-	27 Apr 72	
5	Real Estate	-	11 Jan 72	28 Mar 72
6	Hydraulic Analysis	Dec 70		
7	*Detailed Design of Structures	-	31 Aug 71	
8	Site Geology	-	6 Nov 70	11 Jun 71

* Supplement submitted 19 Apr 72

14 March 1972

FINAL PROGRESS REPORT
TRUMBULL POND DAM

PART I: ULTIMATE STRAIN CAPACITY TESTS

Purpose and Scope

1. The purpose of this investigation was to obtain information as to the physical characteristics, particularly ultimate strain capacity, of concrete containing the aggregate under consideration and to use these results in developing a realistic control plan for Trumbull Pond Dam.

2. The modulus of elasticity and compressive strength of the aggregate and heat of hydration of the cement were determined. Concrete properties determined included compressive and tensile splitting strengths, thermal diffusivity, specific heat, adiabatic temperature rise, coefficient of thermal expansion, uniaxial creep, and ultimate strain capacity. In addition, concrete specimens were fabricated for exposure at Treat Island Exposure Station.

Materials and Mixtures

3. All materials were furnished by the New England Division. Pit-run sand and gravel from an undeveloped onsite source were laboratory processed to meet gradation requirements of CE 1401.01, April 1971 Standard Guide Specifications for Concrete. Rock cores, 2 by 4 in. nominal, were drilled from selected pieces of aggregate. These cores were sawed and ends ground prior to mounting two longitudinal strain gages, diametrically opposite, on each specimen. Cores were then tested to determine compressive strength and modulus of elasticity. Results of individual tests and a brief description of each core are given in table 1. Compressive strength results ranged

from 5100 to 26,670 psi with an average of 16,370 psi. Values of the modulus of elasticity ranged from 2.90 to 7.44×10^6 psi with an average of 5.76×10^6 psi.

4. Atlas type II portland cement shipped from the Hudson, New York, plant was used in this investigation. Chemical and physical properties of the cement as determined by the manufacturer are given in table 2. The heat of hydration of the cement, determined in accordance with CRD-C 229, was 69 and 77 cal/g at 7 and 28 days age, respectively. The pozzolan replacement material used in this investigation was a fly ash manufactured in Connecticut. Darex, triethanolamine salt of a sulfonated hydrocarbon, was used as the air-entraining admixture.

5. Mixture proportions for two mass interior concretes (6-in. MSA), one with 35 percent fly ash replacement of cement (PF) and one with no cement replacement (P), were furnished by New England Division as follows.

<u>Material</u>	<u>Solid Volume, cu ft</u>		<u>SSD Weights, lb</u>	
	<u>P</u>	<u>PF</u>	<u>P</u>	<u>PF</u>
Portland cement	1.389	0.979	273	192
Fly ash	--	0.527	--	79
Fine aggregate	6.273	5.642	1045	940
Coarse aggregate	15.357	16.059	2577	2696
Water	2.901	2.740	181	171
Air	<u>1.080</u>	<u>1.053</u>	<u>--</u>	<u>--</u>
	27.000	27.000	4076	4078

Tests of Freshly Mixed Concrete

6. Average physical characteristics of the freshly mixed concrete were as follows.

	Mixture	
	<u>P</u>	<u>PF</u>
Slump, in.*	2	2
Air content, %*	5.1	5.0
Placement temperature, F	52	54

*Portion passing 1-1/2-in. sieve.

Compressive Strength, Modulus of Elasticity, and Poisson's Ratio

7. A total of thirty-six 6- by 12-in. cylinders were fabricated from concrete wet-sieved through the 1-1/2-in. sieve. Four surface strain gages, two each lateral and longitudinal, were mounted on each specimen 1 day prior to testing. Six specimens, three each round, were tested at each of 7, 28, and 90 days age for each concrete mixture. Results, an average of three tests, are as shown in table 3. Compressive strength gain characteristics for the two mixtures, an average of the two rounds, are given in fig. 1.

Splitting Tensile Strength

8. A total of thirty-six 6- by 12-in. cylinders fabricated from wet-sieved concrete were tested in accordance with CRD-C 77 to determine splitting tensile strengths of the two concrete mixtures. Results, an average of three tests, are as shown in table 3. Average splitting tensile strength gain characteristics are given in fig. 2.

Coefficient of Linear Thermal Expansion

9. Four 6- by 16-in. concrete specimens, two each mixtures P and PF, each containing an embedded Carlson strain meter, were fabricated from concrete wet-sieved through a 1-1/2-in. sieve. Upon stripping, the specimens were sealed and stored at 73 F. Beginning at 26 days age the specimens

subjected to temperatures of 40, 60, 85, and back to 73 F. Strain readings were taken immediately prior to removal from storage and then over a 3-day period after subjecting the specimens to 24 hr in the previously mentioned temperatures. Results (fig. 3 and 4) indicate the coefficients of linear thermal expansion to be 5.9 and 5.5 millionths/F for mixtures P and PF, respectively.

Thermal Diffusivity and Specific Heat

10. Four 6- by 12-in. cylinders, two each mixtures P and PF, were fabricated from concrete wet-sieved through a 1-1/2-in. sieve. The average thermal diffusivity of these specimens at 28 days age as determined in accordance with CRD-C 36 was 0.026 and 0.025 sq ft/hr for mixtures P and PF, respectively.

11. At the conclusion of the diffusivity tests, concrete from the four cylinders was used in specific heat tests. Results of these tests conducted in accordance with CRD-C 124 averaged 0.21 btu/lb-deg F for both mixtures.

Adiabatic Temperature Rise

12. The adiabatic temperature rise of each 6-in. MSA concrete mixture was determined in accordance with CRD-C 38. Results (fig. 5 and 6) indicate the temperature rise was 48 and 39 F for mixtures P and PF, respectively.

Uniaxial Creep

13. Eight uniaxial creep specimens, four each mixtures P and PF, each containing an embedded Carlson strain meter, were cast from concrete wet-sieved through a 1-1/2-in. sieve. After stripping, these specimens were sealed and stored at 73 F. Two specimens from each mixture were loaded

incrementally to $0.35 f'_c$ at 28 days age. Initial elastic deformation was 524 and 332 millionths for mixtures P and PF, respectively. Results of periodic strain measurements on these specimens during the loading period and after unloading are shown in fig. 7 and 8.

14. The remaining four specimens were used as controls to determine length changes under static temperature and moisture conditions. Results indicated the volume change under such conditions was essentially the same for both mixtures, an apparent shrinkage of less than 30 millionths at the time creep specimens were unloaded.

15. Curves-of-best-fit based on a least squares analysis were computed as shown in fig. 9 for the creep test data which have been corrected for the appropriate volume changes. As expected, the concrete with a lower modulus of elasticity (mixture PF) exhibited the higher creep.

Ultimate Strain Capacity

16. Twenty-four mass concrete beams (12 by 12 by 66 in.), 12 each from mixtures P and PF, were cast from concrete wet-sieved through a 3-in. sieve. Two rounds of six beams each were cast for each mixture. Concrete materials were precooled to obtain concrete placement temperatures of 50-55 F. Strain meters were positioned in the forms parallel to the top and bottom fibers, 1-1/2 in. from the concrete surface, and centered within the middle third of a 60-in. simple span, prior to concrete placement. All beams were cured in their molds under moist burlap at approximately 72 F for a period of 5 days. Beams were then stripped and sealed to prevent drying during storage and testing. Both rapid- and slow-loading rates were used in testing

these beams under 1/3-point flexural loading. One beam of each round was tested to failure at 7 days age using a conventional rapid-loading rate of 40-psi fiber stress per minute. A second beam was started in its slow-loading cycle at 7 days age and a third beam stored under no load. In the slow-loading cycle, 25-psi fiber stress was applied to the beam weekly until failure occurred. At the time of failure in the second beam, the third beam was then tested to failure using conventional rapid loading. The three remaining beams in each round were tested in the same sequence with testing initiated at 28 days.

17. Individual beam test results on mixture P concrete are shown in table 4. Load-strain data obtained from these tests are contained in fig. 10 and 11. The average tensile strain capacity in the 7-day slow-loading tests (118 millionths) was 1.84 times that obtained in the rapid-load tests (64 millionths) at 7 days age. Beams tested in rapid loading the same day companion beams failed in the slow-loading tests had an average tensile strain capacity of 88 millionths. This represents an increase in strain capacity, slow versus rapid loading, of 1.34 times. These results indicate the 54 millionths increase in strain capacity, slow loading compared to rapid loading at 7 days age, could be attributed to both the increased maturity (30 millionths) and creep in the concrete (24 millionths).

18. The average tensile strain capacity of mixture P concrete, in 28-day slow-loading tests (102 millionths) was only 1.15 times more than that obtained in the rapid-load tests (89 millionths) at 28 days age. Beams tested in rapid loading the same day companion beams failed in the slow-

loading tests had an average tensile strain capacity of 78 millionths, less than that obtained in the 28-day rapid-load tests, even though the modulus of rupture had increased by approximately 6 percent. This indicates an increase in strain capacity, slow versus rapid loading, of 1.31 times, essentially the same increase obtained in the earlier age tests. This indicated increase must be attributed primarily to creep in the concrete since the more mature concrete (92 and 131 days age) actually exhibited a decrease in strain capacity when compared to concrete of 28 days age.

19. Individual beam test results on mixture PF concrete are shown in table 5. Load-strain data are shown in fig. 12 and 13. The average tensile strain capacity in the 7-day slow-loading tests (88 millionths) was 1.69 times that obtained in the rapid-load tests (52 millionths) at 7 days age. Beams tested in rapid loading the same day companion beams failed in the slow-loading tests had an average tensile strain capacity of 73 millionths. This represents an increase in strain capacity, slow versus rapid loading, of 1.21 times. The increase in strain capacity, slow loading compared to rapid loading at 7 days age, is due, as in the mixture P concrete, to both increased maturity (21 millionths) and creep of the concrete (15 millionths).

20. The average tensile strain capacity of mixture PF concrete in 28-day slow-loading tests (80 millionths) was 1.23 times that obtained in the rapid-load tests (65 millionths) at 28 days age. A beam tested in rapid loading the same day a companion beam failed in the slow-loading test had a tensile strain capacity of 74 millionths. This represents an increase in strain capacity, slow versus rapid loading of only 1.08 times. As in

the earlier age test, this small indicated increase is attributed to increased maturity (9 millionths) and creep (6 millionths) of the concrete.

21. Averaging the rapid-load test results for both mixtures indicates the tensile strains to be slightly higher than the compressive strains at failure, with the larger difference, associated with mixture P concrete, being less than 10 percent. The slow-load tests indicate the compressive strains are somewhat higher than tensile strains at failure with average differences of approximately 25 and 50 percent for mixtures P and PF, respectively. Results of strain measurements on the beams in storage (fig. 14 and 15) indicate this difference is due to autogenous shrinkage. If the results of the slow-load tests are corrected for this shrinkage as shown in table 6, the average compressive and tensile strains are essentially the same for a given mixture.

22. The apparent increases in tensile strain capacity, slow versus rapid loading, were somewhat low, averaging only 1.14 and 1.32 times for mixtures PF and P, respectively. Although the significance of the small difference is questionable, it is somewhat surprising to note that the larger increase was associated with the concrete exhibiting the lower specific creep. Apparently the rate of increase in elastic modulus of the mixture PF concrete (fig. 16) and resultant increase in stiffness had more effect on the strain capacity than the slightly higher creep of this concrete.

23. The average tensile strain capacity determined in slow-loading tests was larger for both mixtures in tests initiated at 7 days age than

similar tests initiated at 28 days age. Since for a given mixture, the average modulus of rupture at failure was essentially the same for both loading ages, this illustrates how the increased stiffness of the concrete at later ages tends to reduce the strain capacity for a given stress level. A similar effect can be observed in the rapid-load tests. The modulus of rupture of mixture P concrete appears to approach an upper limit at 80-100 days age (fig. 17) whereas the mixture PF concrete exhibits a continuous increase. The relatively small increase in stiffness of mixture P concrete (fig. 16) in combination with essentially no increase in stress capacity beyond 80 days results in a reduced tensile strain capacity (fig. 18). In comparison, the increased stress capacity of the mixture PF concrete results in an increased tensile strain capacity in spite of the increased beam stiffness. Results of these tests indicate the desirability of conducting similar tests at more advanced ages.

24. While the tensile strain capacity was generally increased by slow-load application, stress capacity or tensile strength of comparable beams was essentially the same for both types of loading.

PART II: THERMAL STUDIES

25. Strain gradients in mass concrete structures are produced mainly by thermal gradients, autogenous shrinkage, and drying shrinkage. This study is concerned with the prediction of thermal strains produced by internal heat generation, external ambient temperature changes, and when precooled concrete is placed on older warm concrete. This information will be used to help in development of a temperature control plan during construction aimed toward minimizing thermal cracking.

Finite Element Computer Code

26. A two-dimensional finite element computer code, developed originally by Dr. Edward L. Wilson of the University of California at Berkeley, revised by the Walla Walla District, and recently revised for use by the Waterways Experiment Station (WES), was used in this parameter study.

Method of Calculation

27. The computer code incrementally places concrete in lift thicknesses and with lift placement times as prescribed by the user. The concrete temperature variation is calculated by utilizing the thermal properties of the concrete to govern the heat flow within and in or out of the structure due to the ambient temperature conditions, hydration heat generated, and placement temperature conditions. Several calculation increments are made during each lift cycle to more accurately describe the internal temperature at various times during the construction simulation.

Variable Control Parameters Used.

28. This study was designed to simulate construction with various values of the following control parameters.

- a. Placement temperatures: 50, 55, and 60 F.
- b. Lift thickness: 5, 7-1/2 ft.

- c. Cement factor: 2.75, 3.25 bag/cu yd.
- d. Insulation: none, 0.50 μ , and 0.25 μ .
- e. Ambient temperature conditions: mean ambient and 4-day sustained temperature drops of 20 F at 37.5, 39.5, and 53 days into construction.
- f. Slipform rates: 5, 10, 20 in./hr.

Finite Element Model

29. A cross-section of the dam at Station 3+20, that of maximum size, was used in this study (fig. 19). Since it was found that maximum temperatures develop in the lower section of a structure having this configuration, only the lower section was studied in order to reduce total computer time. A finite element model (fig. 20) was designed to show greater detail both vertically and horizontally at the 20-40 ft level. Thus, points at which temperatures were calculated were as close as 4 in. to the upstream face, 2 ft to the downstream face, and at 2.5 ft intervals vertically between the 20-60 ft levels except at the 35-40 ft level where the interval was 1.25 ft. This allowed thermal gradients to be plotted more accurately in areas where the gradients were extremely nonlinear.

Ambient Temperature

30. Four ambient temperature histories were used in this study (fig. 21). History No. 1 was determined from the monthly mean temperatures for Bridgeport, Connecticut, for the time between 1 August and early December. Histories No. 2-4 were produced by imposing a 20 F temperature drop on history No. 1 at 37.5, 39.5, and 53 days, respectively, and sustaining the drop for 4 days before returning to follow history No. 1. In all cases, the temperature drop took place over a 6-hr period.

Time at Beginning of Simulations

31. All computer simulations began construction on 1 August. Actually, the first concrete was placed at the beginning of the second day as one day was allotted for foundation temperatures to equilibrate between ambient temperature and a constant foundation temperature of 70 F at a depth of 5 ft. Hereafter, the times referred to in this text will be elapsed time into the simulation except where specifically stated otherwise, i.e., when time after particular lift placement is discussed.

Insulation

32. The three conditions of insulation used in this study had 1.0 μ (no insulation), 0.50 μ , and 0.25 μ heat conduction factors, respectively. When insulation was used, it was placed on all exposed surfaces at placement time. Insulation was not removed from vertical surfaces while insulation was kept on horizontal surfaces from the time of placement of one lift to the time of placement of the next lift.

Concrete Properties

33. Table 7 lists the properties, described earlier, of the two concrete mixtures used in the computer simulations along with those of Dworshak, Libby, and Clarence Cannon Dams for reference and comparison. Adiabatic temperature rise plots are shown in fig. 5 and 6.

Computer Simulation of Construction

34. A listing of the control parameters of each computer simulation is shown in table 8. Since the number of simulation runs would have been excessive if each variable was tested independently, it was determined that the particular set of runs shown in table 8 would provide sufficient

information upon which to base consideration for a temperature control plan for Trumbull Pond Dam.

35. The 5-ft lift thickness was utilized as the standard upon which to examine the variable of placement temperature, insulation, sustained ambient temperature drops, cement factor, and combinations thereof. The concrete for all 5-ft lift runs and the 7-1/2-ft lift run was placed to a height of 65 ft in the first construction stage. At 5-day intervals between placement of successive lifts, 5-ft lift construction took 60 days and 7-1/2-ft lift construction took 45 days to reach the 65-ft level. In both cases the simulations were continued 15 additional days to allow temperatures to peak at the 35-40-ft level.

36. Slipform construction was accomplished by placing individual element rows successively. Ideally, concrete would be placed and vibrated continuously; however, construction would likely follow procedures of placing approximately 20-in. layers during which concrete would be vibrated before the next layer was placed. The rate of layer placement would be adjusted to the particular slipform construction rate. Since the element height varied, as can be noted in fig. 20, the slipform simulations were not conducted with a constant layer height increment. Consequently, each elemental row was placed with a sufficient delay in construction after placement of the previous row to equal the slipform rate. The elemental row height between the 20- and 60-ft levels more closely approximates an actual slipform layer. Concrete was placed continuously to a height of 50 ft. Then, a 21-day interval was programmed before resuming construction to the 65-ft level.

Discussion of Results

37. Since the bulk of the parameter study was accomplished with 5-ft lift placement, these results and their implications upon potential thermally induced cracking will be discussed first. Then, the results of runs in which the placement rate was varied will be discussed.

Five-Foot Lifts - Peak Temperatures

38. The peak temperatures reached in the 10 runs in which 5-ft lifts were used are listed below.

Run No.	Mixture No.	Ambient History No.	Insulation, μ (1.0 μ = none)	Temperature, F	
				Placement	Peak
1	PF	1	1.0	50	87.8
2	PF	1	1.0	55	90.8
3	PF	1	1.0	60	92.6
4	P	1	1.0	50	92.6
5	P	1	1.0	60	98.6
6	PF	2	1.0	50	87.7
7	PF	2	0.5	50	88.8
8	PF	2	0.25	50	88.9
9	PF	3	1.0	50	87.7
10	PF	4	1.0	50	87.7

Comparing runs 1-3 and 4-5, the well-known fact that placement temperature and cement factor strongly affect peak temperatures is shown. Figure 22 depicts typical temperature rise at the center of the section for Mixture "P" placed at 50 and 60 F. Runs 1, 6, 9, 10 show that a 20 F ambient temperature drop sustained for 4 days when mean ambient temperatures are approximately 60-70 F does not affect peak temperatures. By adding insulation and comparing runs 1, 7, and 8, we find the peak temperature rise to fit the adiabatic heat released. Thus, in a massive structure the central area is affected very little by external parameter variations. Any differences which do occur are near the surface.

Five-Foot Lifts - Near Surface Thermal Gradients

39. Figure 23 shows typical thermal gradients using concrete placed at 50 and 60 F. These gradients are taken along a line I-D (fig. 20) at

38 and 53 days. It can readily be seen that it will take longer to reach a near-linear gradient as placement temperatures are increased. Since a linear thermal gradient is most desirable in controlling thermal cracking, it is apparent that higher placement temperatures will keep a massive structure in a potential cracking situation for a longer time.

40. Lift No. 8, placed at 36 days into construction, was chosen to study thermal gradients under various ambient temperature variations and insulation conditions. Thermal gradients near a vertical surface as described here were taken at the midpoint of lift 8 (37.5 ft). Figures 24-27 show thermal gradients calculated with and without the imposition of ambient temperature variations and the effects of using insulation. The most critical time for a severe drop in ambient temperature seems to be approximately 2 days following placement, primarily because hydration temperature rise has reached 40-50 percent of peak with little time elapsed to allow near-surface dissipation of this heat. Although the modulus of elasticity is low and creep potential is high at early times, the strain capacity is quite low. At 2 days after placement, the temperature is almost constant along a horizontal plane through the monolith. If at this time the ambient temperature is lower than the average temperature in the lift and a severe drop in ambient temperature occurs (for this example, 20 deg/6 hr), a steep thermal gradient is produced near the surface which can approach the strain capacity of the concrete. Figure 29 shows a comparison of the thermally induced strain in the surface layer (1 in. dept.) assuming 100 percent restraint versus age of the concrete for a 20 F drop in ambient temperature occurring at 1.5 and 3.5 days after placement. The strain capacity for mixture PF is plotted for comparison. At 2 days age

and one-half day following the temperature drop, the thermal strain approaches the strain capacity. No insulation was used in this comparison. When insulation was used under identical conditions, the unit strain is not close to being excessive.

41. Thermal strains can be minimized through the use of insulation which lowers the time-rate of change of temperature at the surface of the concrete and thus holds the thermal gradient in the concrete near the surface within acceptable limits. Figures 30 and 31 show the effect of temperature drop on surface and near surface concrete with and without insulation. These data show that for a drop of 20 F in air temperature, the reduction in surface temperature can be held to a safe level (2 to 8 deg per 5-day interval) by using insulation having thermal conductances ranging from 0.25 to 0.50 BTU per hr-ft²-F.

42. Upon examining thermal gradients normal to the horizontal exposed surface at the top of a lift, they were found to correspond to those normal to the vertical surfaces when similar exposure and insulation conditions existed. A typical isotherm plot of the dam is shown in fig. 28.

Five-Foot Lifts - Lift Interface Thermal Gradients

43. When a lift has been exposed to ambient temperatures markedly higher than placement temperature and a new lift is placed upon it, severe tensile strains can occur in the older lift.* Figure 32 depicts the vertical thermal gradients along line ABCDEFG, fig. 20, for run No. 1. Times represented by each gradient are those at each new lift immediately prior.

* Raphael, Jerome M. and Wilson, Edward L., "Maximum Temperature Stresses in Dworshak Dam," Structural Engineering Laboratory, University of California at Berkeley, July 1967.

to placing the next lift. In each lift except lift 1 prior to placement of lift 2, the near-surface concrete is already in tension due to the existing thermal gradient. When the next lift is placed at 50 F, the temperature of the old lift surface will drop suddenly to equilibrate with the temperature of the newly placed concrete. Additional tensile strains will result in the older lift since the older concrete has acquired a substantial portion of its ultimate modulus of elasticity and creep potential has lessened, localized restraint is increased. Thus, a rapid increase in tensile stress produced by the additional tensile strain will occur. For example, note the thermal gradient in fig. 32 at lift 7 at 36 days. This is just prior to placing lift 8. The concrete in lift 7 has 5 days age. When lift 8 is placed, the lift 7 surface will immediately drop from near 70 F to approximately 60 F. Figure 33 depicts the thermal gradient in lift 7 prior to and 1 hr after placement of lift 8. The first inch adjacent to the new interface will experience a temperature differential of approximately 6 F. Assuming 100 percent restraint, this will produce a tensile strain of approximately $33\mu\text{in.}$ in concrete with a strain capacity near $44\mu\text{in./in.}$ Since the surface of lift 7 was already in tension, the additional tensile strain may cause the total tensile strain to exceed the strain capacity. In any case, the older concrete is subjected to a tensile strain which is a substantial proportion of strain capacity. Any other effects such as normal, localized weaknesses in the concrete may cause cracking in the older concrete.

44. The concrete in the new lift is in a plastic state at placement time, thus, will not provide restraint to the old lift and will not itself have the ability to crack. If, at a later time, the concrete in the new

lift goes into tension, a crack formed in the previous lift can be propagated into the new concrete. This cracking can occur due to stress concentrations at the crack zone because of a lack of interface restraint at that spot. Cracks thus formed can propagate through an entire structure as the stress conditions change with time and further construction.

Seven and one-half Foot Lifts

45. Simulation run No. 11 was made using a lift height of 7-1/2 ft. This run was conducted under the same conditions as run No. 1 with 5-ft lifts. A peak temperature of 89.0 F was reached compared with 87.8 F from run No. 1. Figure 34 shows the variation in temperature rise at the same point in the monolith under various placement rates, but with all other parameters held constant. The higher peak temperature for 7-1/2-ft versus 5-ft lift construction is due to decreased heat flow out of each lift during the interval between placement of adjoining lifts because fewer lift surfaces are exposed. Peak temperature rise equals that reached under adiabatic conditions. For comparison, fig. 35 shows thermal gradients at 7 and 28 days after placement for 5- and 7-1/2-ft lift construction at the 37.5-ft height. The gradients are very similar with the only difference being near the surface because ambient conditions were slightly different at time of placement. There appears to be little difference between the use of 5- and 7-1/2-ft lifts with 5-day intervals between lifts except that 7-1/2-ft lift construction produces peak temperatures approximately 1 deg F higher.

Slipform Construction

46. Run No. 12-14 simulated slipform construction at 5, 10, and 20 in./hr, respectively. Except for placement rates, these runs were made under the same conditions as runs 1 and 11. Figure 34 shows the peak

temperature rise for the three slipform runs for comparison with runs 1 and 11, 5- and 7-1/2-ft lift construction, respectively. Immediately evident is that the peak temperatures reached were inversely proportional to the slipform construction rate and were all higher than that of adiabatic rise. In observing the rate of temperature rise in each succeeding layer, it was noted that this rate became incrementally higher as construction progressed. The amount of heat flow out of exposed surfaces is low at early times yet the hydration rate is highest. Thus, at more rapid rates of placement such as in slipform construction, each incremental lift experiences an initial accelerated hydration rate. As the placement rate is increased over 5 in./hr, less time is allowed for each incremental lift to gain hydration heat from the previous one. Essentially, a condition approaching instantaneous placement of the monolith is reached where temperature rise will be adiabatic. At very low placement rates such as 5- and 7-1/2-ft placement at 5-day intervals (0.50 and 0.75 in./hr, respectively), the peak temperature rise again corresponds to adiabatic rise. Figure 36 demonstrates the differences in peak temperature when compared to placement rate. The dashed line was inserted to show that the possibility exists for a single placement rate to produce a maximum peak temperature for a particular set of placement parameters.

47. The variation of thermal gradients with slipform placement rate is shown in fig. 37 at 7 and 28 days after placement at the 37.5-ft level. These gradients can be compared with those shown in fig. 35 for 5- and 7-1/2-ft placement at the same times after placement and similar position. Figure 38 shows the construction plan for all runs made. From this figure, a comparison of placement times at the 37.5-ft level can be made. In comparing slipform and conventional construction in this study, it should be recognized

that the bulk of slipform placement occurred within several days of initial construction whereas conventional construction was accomplished over a longer time. Because the ambient temperature was gradually decreasing with time, the conditions for heat flow were different during the 28-day hydration period for the two methods. Data appear to show, however, that early age strain gradients will be steeper and maximum total strain will be higher when using slipform construction. Strain gradients calculated after several weeks following placement should generally have similar slopes for both methods of construction.

Conclusions and Recommendations

48. Based on the results of this investigation, the following are conclusions reached and recommendations made toward establishment of a temperature control plan for Trumbull Pond Dam.

49. Concrete Mixture PF appears best since it produces peak temperatures approximately 10 F lower than Mixture P under similar placement conditions. Thus, considering a thermal coefficient of expansion of 5.5 μ in. per degree F and assuming 100 percent restraint, Mixture PF will undergo a total strain differential of 55 μ in. less than Mixture P. This would appear to more than offset the higher strain capacity of Mixture P. In addition, if a total temperature drop of 45 F is used as a design control and 46 F is the final equilibrium temperature of the dam, the 98 F peak temperature produced by Mixture P will be several degrees higher than allowable.

50. Results showed that the differences between the use of 5- and 7-1/2-ft lifts with 5-day placement intervals are small. This is the case when comparing both near-surface thermal gradients and peak temperature rise. By increasing the placement interval from 5 to 7 days with 7-1/2-ft

lifts, the differences between 5- and 7-1/2-ft lift placement would be reduced due to an increase in heat flow out of the structure during construction. The use of 7-1/2-ft lifts will reduce the number of lift surfaces that will be placed in tension when the surface temperature versus placement temperature differential is high. Thus, the number of possibilities for interface cracking is reduced.

51. The use of insulation was found to be complex. Because of the large number of parameters studied, the number of runs using insulation was limited. Results indicated that in most cases an insulation conductance factor of 0.5_{μ} BTU per $\text{hr-ft}^2\text{-F}$ would satisfactorily retard near-surface heat flow during periods of a rapid drop in ambient temperature. The use of insulation conductance factors less than 0.5_{μ} would seem to be required when the drop in ambient temperature was extreme (30-50 F), took place in a short period of time, and was sustained for long periods of time.

52. The temperature control of lift surfaces was found to be the most critical. Exposed lift surfaces allowed to remain at temperatures much higher (20-30 F) than placement temperatures will experience potentially dangerous thermal shock when the cooler concrete is placed upon it. This situation is worse than exposing a surface to a comparable drop in ambient temperature because the surface and near-surface cooling will be more rapid with direct application of a solid than with air. Practices should be followed in which the exposed surface is cooled slowly before placement of a successive lift to reduce thermal shock.

53. A consideration which should be explored is the use of a higher placement temperature in the first 20-in. layer of a lift which is placed

on relatively warm concrete. Obviously, this practice would make construction procedures more difficult; however, this practice will produce a less extreme thermal gradient in the older lift without substantially raising peak temperatures. This practice might be incorporated when high ambient temperatures and the use of insulation have kept lift surface temperatures much higher than normal placement temperature. Any increase in peak temperature thus produced can be reduced by allowing a longer time interval between lifts or if the ambient temperature is high by cooling the surface for several days before placement of the next lift.

54. The contribution of solar effects was not studied in this investigation, but does require some thought. It is very important to reduce solar heating in concrete especially at set times and at early age. If surfaces of fresh concrete are exposed to solar radiation either directly or by conduction from formwork and allowed to rise, a reverse thermal gradient can exist at a zero stress level. That is, the concrete surface temperatures are higher than interior temperatures at and immediately after set. At later times when hydration progresses and surface temperatures drop, the near-surface concrete will experience additional tensile strains. The insulation selected should have low absorption capacity for infrared and ultraviolet radiation. Experience at Libby Dam appears to indicate that the concrete underlying a layer of insulation reached temperatures near 100 F due mainly to ultraviolet solar radiation.

55. The results of slipform simulation runs at three rates of construction indicated that peak temperatures would be 5 to 8 F higher than by conventional construction methods. Near-surface thermal gradients produced by slipforming would be slightly more severe at early age, but comparable to

conventional construction after several weeks age. The only long time difference would be a greater surface to internal temperature difference with slipforming due to the increased peak temperature. The problem of interface cracking would be greatly reduced because temperature differences and elastic properties between placed concrete and additional concrete would be small. Thus, any substantial interface strains would be greatly reduced. The number of computer simulations of the slipform method was not sufficient to study the effects of the method in detail. However, since it is probable that most substantial thermal cracking occurs at lift interfaces, it would appear to be a promising method for mass construction.

Table 1

Rock Cores - Trumbull Pond Dam

<u>Specimen No.</u>	<u>Diameter in.</u>	<u>Length in.</u>	<u>Ultimate Load, lb</u>	<u>L/D</u>	<u>Compressive Strength psi</u>	<u>Modulus of Elasticity psi x 10⁶</u>	<u>Description</u>
I-2	1.95	3.96	49,100	2.03	16,420	6.35	Quartz diorite gneiss with small amount of hornblende and garnet with a schistose inclusion which is predominantly biotite, chlorite, plagioclase, with small amount of hornblende and garnet. Core is medium grained with a crude high-angle foliation.
I-3	1.95	3.93	21,250	2.02	7,110	6.77	Biotite schist with garnet and chlorite--approaching a gneissic texture. Core is medium grained with a near vertical foliation. Sample is similar to inclusion in I-2.
II-1	1.95	3.65	49,500	1.87	16,560	6.71	Quartz diorite gneiss with a well defined high-angle foliation. Foliation is defined by large plagioclase stringers and biotite. Matrix is medium grained.
II-2	1.95	3.40	60,500	1.74	20,230	6.19	Quartz diorite gneiss similar to II-1 but has more biotite and fewer plagioclase stringers. Foliation defined by biotite is similar to II-1.
II-4	1.95	3.96	39,800	2.03	13,310	5.71	Quartz diorite gneiss similar to II-1 but has a better developed foliation and fewer plagioclase stringers similar to II-2. Core is iron strained. Has a near vertical foliation.

(Continued)

(Page 1 of 3)

Rock Cores - Trumbull Pond Dam (Continued)

<u>Specimen No.</u>	<u>Diameter in.</u>	<u>Length in.</u>	<u>Ultimate Load, lb</u>	<u>L/D</u>	<u>Compressive Strength psi</u>	<u>Modulus of Elasticity psi x 10⁶</u>	<u>Description</u>
II-5	1.95	3.98	27,400	2.04	9,160	7.30	Biotite, quartz diorite gneiss similar to II-1 with more biotite. Foliation is not as steep as II-1-4, in this core about 45-50 deg.
III-1	1.95	3.97	58,600	2.04	19,600	6.86	Biotite gneiss with stringers of quartz and feldspar, with a poorly developed high-angle foliation. Core is medium grained.
III-2	1.95	3.45	74,500	1.77	24,920	6.97	Quartz diorite gneiss with a small amount of biotite defining a low-angle foliation--~30 deg. Core is uniformly medium grained.
III-3	1.95	4.04	47,500	2.07	15,890	2.99	Quartz diorite gneiss--appears to be weathered equivalent of III-2--has poorly defined horizontal foliation.
III-4	1.95	3.42	36,100	1.75	12,070	2.90	Biotite gneiss--appears to be finer-grained equivalent of III-1; has a near horizontal foliation.
III-5	1.95	3.31	15,250	1.70	5,100	3.06	Fine-grained biotite gneiss with numerous fractures ranging from horizontal to near vertical. Core has a disrupted near vertical foliation. Sample contains less quartz and and feldspar than III-1-4.

(Continued)

Rock Cores - Trumbull Pond Dam (Continued)

<u>Specimen No.</u>	<u>Diameter in.</u>	<u>Length in.</u>	<u>Ultimate Load, lb</u>	<u>L/D</u>	<u>Compressive Strength psi</u>	<u>Modulus of Elasticity psi x 10⁶</u>	<u>Description</u>
IV-1	1.95	3.95	64,250	2.03	21,480	6.40	Coarse to medium grained quartz diorite similar to I-2 but lacks foliation and metamorphic assemblage. Core is partially iron stained.
IV-2	1.95	3.95	75,750	2.03	25,330	7.44	Medium-grained quartz diorite gneiss similar to I-2 and has a poorly developed high-angle foliation. Biotite is concentrated in clots.
V-2	1.95	3.97	34,800	2.04	11,640	4.14	Coarse-grained quartz diorite gneiss with numerous porphyroblasts of feldspars up to 2 in. in diameter. Core has a crude high-angle foliation.
V-3	1.95	3.18	79,750	1.63	26,670	6.70	Medium-grained quartz diorite gneiss with a well-developed horizontal foliation.

Table 2

Chemical and Physical Properties of Type II
Portland Cement (Lab No. RC-654)

<u>Test</u>	<u>Results</u>
<u>Chemical Data</u>	
SiO ₂ , %	22.4
Al ₂ O ₃ , %	4.38
Fe ₂ O ₃ , %	3.30
CaO, %	63.9
MgO, %	1.5
SO ₃ , %	2.7
Loss on Ignition	1.2
C ₃ S, %	48.0
C ₃ A, %	6.1
<u>Physical Data</u>	
Specific Surface, sq cm/g	
Wagner	1969
Blaine	3629
Soundness, Autoclave Expansion, %	0.00
Time of Setting, hr: min	
Initial	3:15
Final	6:10
Air Content, %	9.7
Compressive Strength, psi	
3 Days	2530
7 Days	3200

Table 3

Concrete Properties - Trumbull Pond Dam

<u>Mix No.</u>	<u>Round No.</u>	<u>Age Days</u>	<u>Comp Strg psi</u>	<u>Tensile Splitting psi</u>	<u>Elastic* Modulus psi x 10⁶</u>	<u>Poisson's Ratio**</u>
PF	1	7	980	120	1.57	0.13
		28	1780	210	1.63	0.14
		90	2590	275	2.47	0.17
	2	7	940	115	1.34	0.12
		28	1910	215	2.07	0.15
		90	2530	270	2.55	0.14
P	1	7	1730	185	2.31	0.13
		28	2680	285	2.54	0.15
		90	3520	365	2.63	0.17
	2	7	1830	215	2.26	0.14
		28	3350	305	2.44	0.17
		90	3640	365	2.80	0.16

* Secant modulus - 50 percent ultimate strength.

** 50 percent ultimate strength.

Table 4

Results of Ultimate Strain Capacity Tests, Mixture P

Round No.	Beam No.	Testing Age days	Loading Rate	Modulus of Rupture,* psi	Strain,** millionths	
					Tension	Compression
1	P-1-1	7	40 psi/min	180	59	54
	P-1-2	7	25 psi/week	270	102	139
	P-1-5	86	40 psi/min†	295	77	79
2	P-2-2	7	40 psi/min	185	69	65
	P-2-1	7	25 psi/week	315	134	154
	P-2-5	99	40 psi/min†	310	99	81
1	P-1-3	28	40 psi/min	250	82	74
	P-1-4	28	25 psi/week	245	89	105
	P-1-6	92	40 psi/min†	265	74	74
2	P-2-3	28	40 psi/min	265	96	77
	P-2-4	28	25 psi/week	335	115	156
	P-2-6	131	40 psi/min†	280	82	79

* Determined at 90 percent of ultimate load.

** Extrapolated outside fiber strain at 90 percent of ultimate load.

† Beams tested under rapid loading same day companion beam failed in slow-loading test.

Table 5

Results of Ultimate Strain Capacity Tests, Mixture PF

Round No.	Beam No.	Testing Age days	Loading Rate	Modulus of Rupture,* psi	Strain,** millionths	
					Tension	Compression
1	PF-1-1	7	40 psi/min	125	53	47
	PF-1-2	7	25 psi/week	245	85	132
	PF-1-5	79	40 psi/min†	250	75	70
2	PF-2-2	7	40 psi/min	120	50	46
	PF-2-1	7	25 psi/week	245	92	138
	PF-2-5	78	40 psi/min†	235	71	75
1	PF-1-3	28	40 psi/min	165	65	55
	PF-1-4	28	25 psi/week	245	77	119
	PF-1-6††	108	40 psi/min†	--	--	--
2	PF-2-3	28	40 psi/min	185	65	64
	PF-2-4	28	25 psi/week	225	82	106
	PF-2-6	92	40 psi/min†	270	74	70

* Determined at 90 percent ultimate load.

** Extrapolated outside fiber strain at 90 percent of ultimate load.

† Beams tested under rapid loading same day companion beam failed in slow-loading test.

†† Beam broken in handling.

Table 6

Autogenous Length Changes, Slow-Load Tests

<u>Beam No.</u>	<u>Shrinkage Strain during Loading Period, millionths</u>	<u>Strain Capacity,* millionths</u>	
		<u>Tension</u>	<u>Compression</u>
P-1-2	20	122	119
P-2-1	21	155	133
P-1-4	9	98	96
P-2-4	12	<u>127</u>	<u>144</u>
	Avg	126	123
PF-1-2	23	108	109
PF-2-1	23	115	115
PF-1-4	13	90	106
PF-2-4	12	<u>94</u>	<u>94</u>
	Avg	102	106

* Extrapolated outside fiber strain determined at 90 percent ultimate load and corrected for autogenous length change.

Table 7

Summary of Inherent Properties of Various Mass Concretes Which Are Considered Important With Regard to Crack Resistance

	Dworshak	Libby	Clarence Cannon		Trumbull Pond	
			Interior	Exterior	Interior PF	Interior P
Strain caused by each 10° F change in concrete temp	55 millionths	60 millionths	50 millionths	50 millionths	55 millionths	59 millionths
Diffusivity	0.04 ft ² /hr	0.067 ft ² /hr	0.051 ft ² /hr	0.049 ft ² /hr	0.025 ft ² /hr	0.026 ft ² /hr
Adiabatic temp rise	40 F	28 F	33 F	42 F	39 F	48 F
Conc strain capacity, 7 days age	70 millionths	40 millionths	40-50 millionths	61 millionths	50-53 millionths	59-69 millionths
Strain capacity, older concrete	80-120 millionths (73-116 days)	78 millionths (90 days)	66-74 millionths (180 days)	61-72 millionths (180 days)	71-75 millionths (78-108 days)	74-99 millionths (86-131 days)
Increase in strain capacity, slow versus rapid loading conc	2.1 times (73-116 days)	1.2 times (28 days)	1.3 times (113-125 days)	1.5 times (161-175 days)	1.14 times (78-108 days)	1.32 times (86-131 days)
Modulus of rupture, 7 days age	145 psi	95 psi	170-205 psi	345-360 psi	120-125 psi	180-185 psi
Modulus of rupture, older concrete	315-400 psi (73-116 days)	250 psi (90 days)	405 psi (180 days)	435-485 psi (180 days)	165-185 psi (28 days)	250-265 psi (28 days)
Sp creep, loading age and duration, 28 days	0.14-0.18	0.11-0.16	0.16	-	0.39	0.36
Sustained modulus of elasticity, 28 days	2.0-2.9x10 ⁶ psi	2.6-3.4x10 ⁶ psi	2.6x10 ⁶ psi	-	1.49x10 ⁶ psi	1.64x10 ⁶ psi
Specific heat		0.22	0.21*	0.21*	0.21	0.21

Note: Strain capacity and modulus of rupture determined at 90 percent of ultimate load

* Assumed value.

Table 8

Computer Simulation Schedule*

<u>Run No.</u>	<u>Lift Height ft</u>	<u>Mixture No.</u>	<u>Ambient History No.</u>	<u>Insulation Factor μ^{**}</u>	<u>Placement Temperature</u>
1	5	PF	1	1.0	50
2	5	PF	1	1.0	55
3	5	PF	1	1.0	60
4	5	P	1	1.0	50
5	5	P	1	1.0	60
6	5	PF	2	1.0	50
7	5	PF	2	0.5	50
8	5	PF	2	0.25	50
9	5	PF	3	1.0	50
10	5	PF	4	1.0	50
11	7-1/2	PF	1	1.0	50
12	Slip form 5 in./hr	PF	1	1.0	50
13	Slip form 10 in./hr	PF	1	1.0	50
14	Slip form 20 in./hr	PF	1	1.0	50

* 5- and 7-1/2-ft lift placed at 5-day intervals.

** 1.0 μ = no insulation

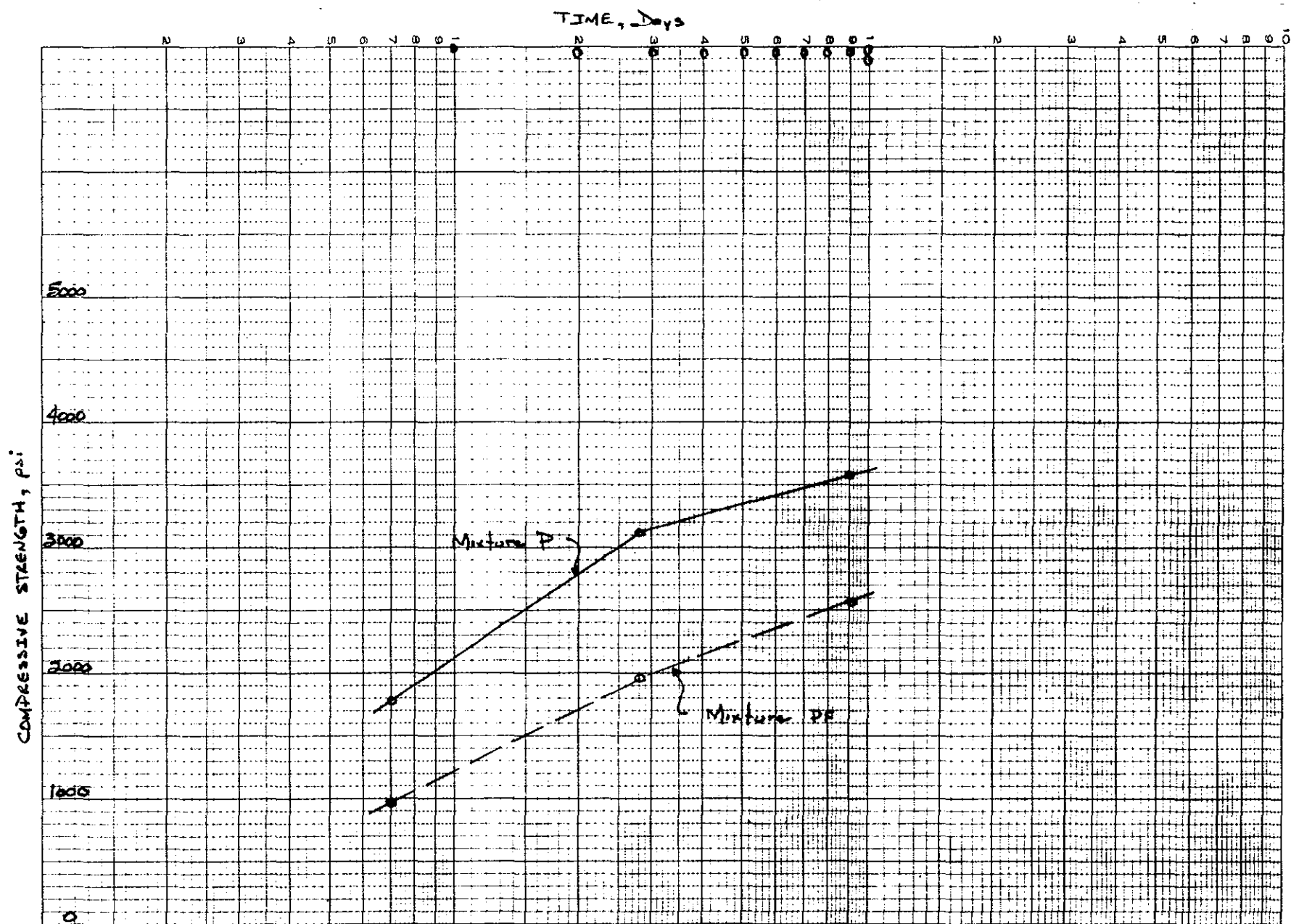


Fig. 1 Compressive Strength Gain

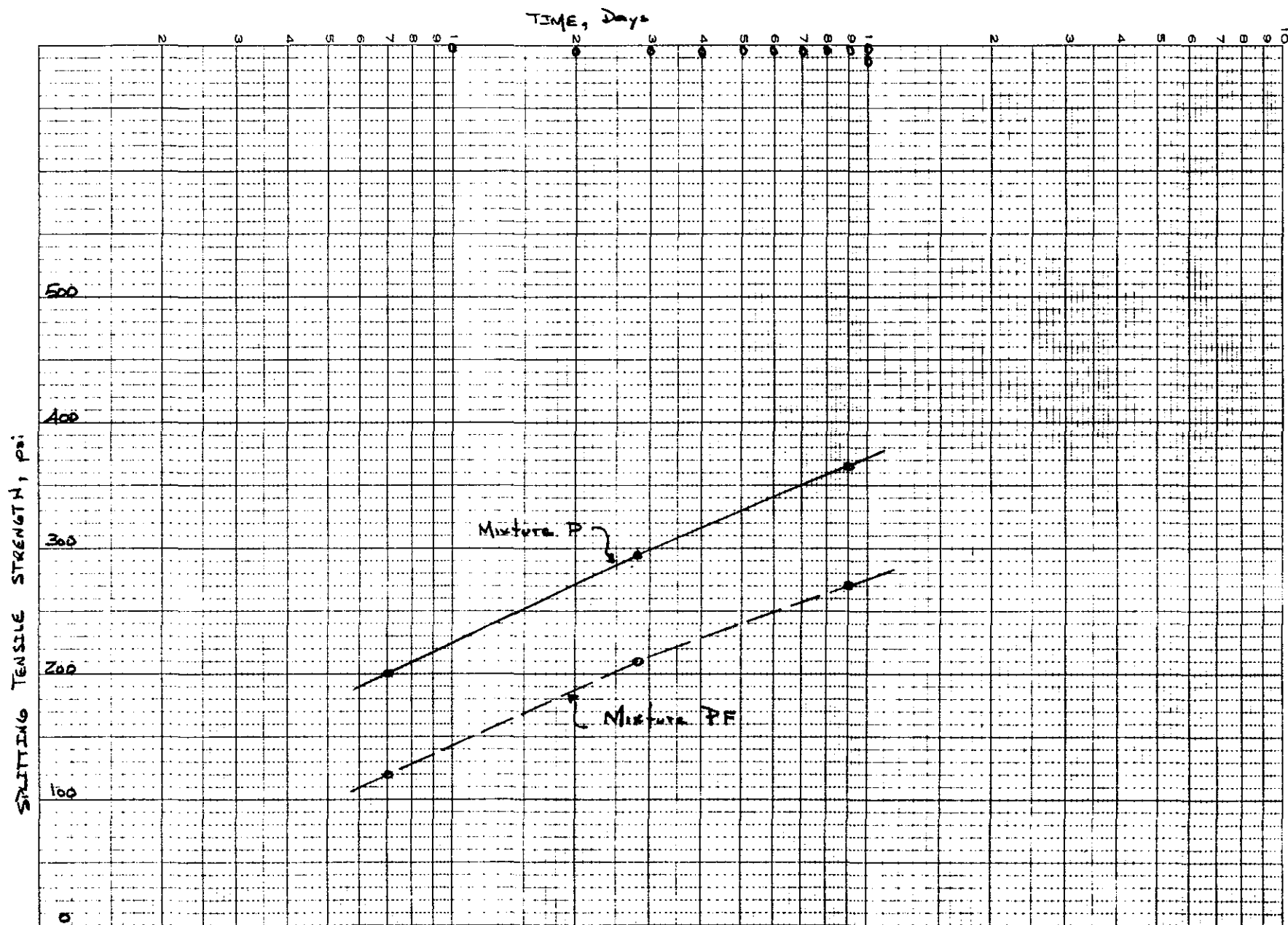


Fig. 2 Splitting Tensile Strength Gain

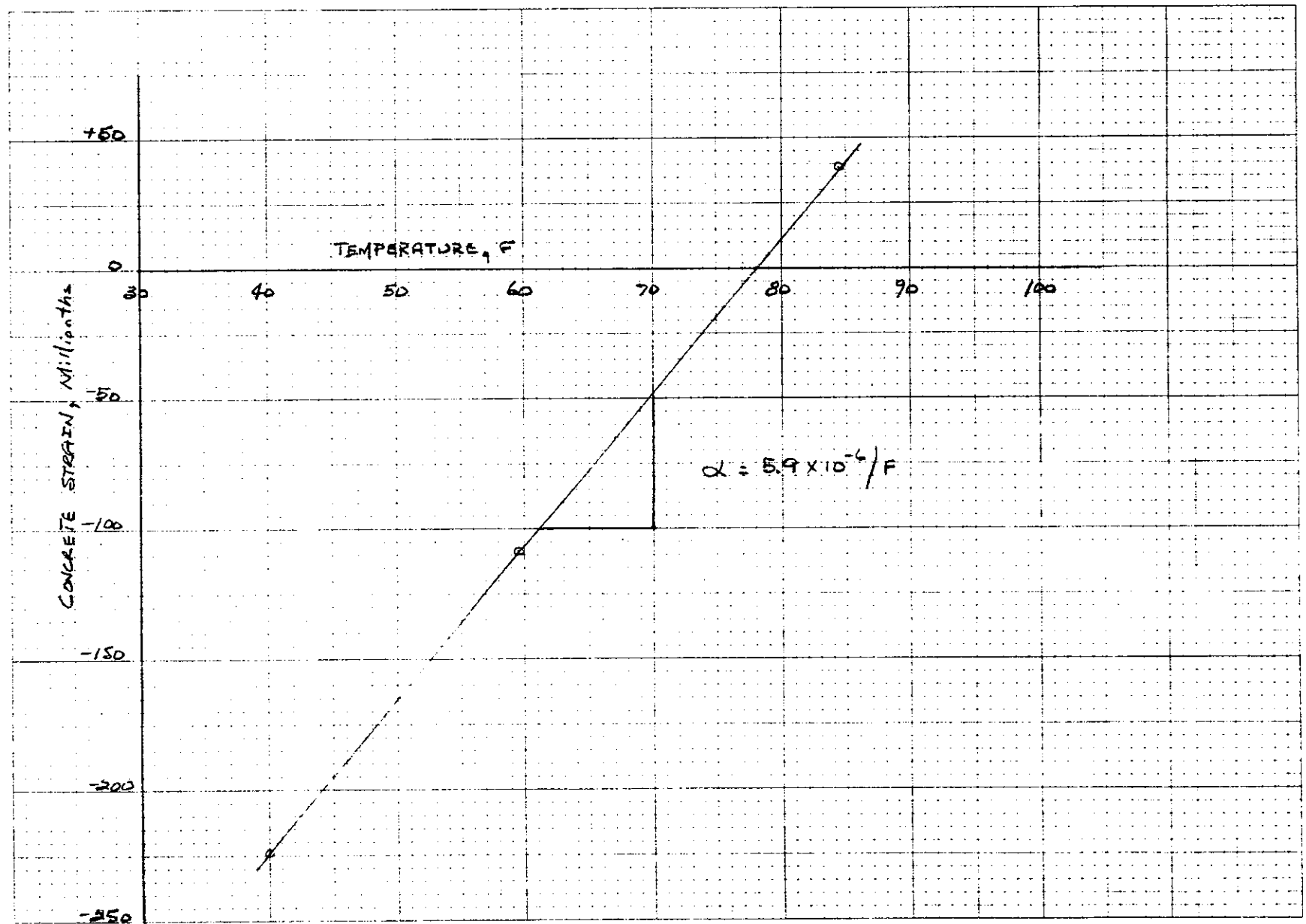


Fig. 3 Coefficient of Linear Thermal Expansion, Mixture P

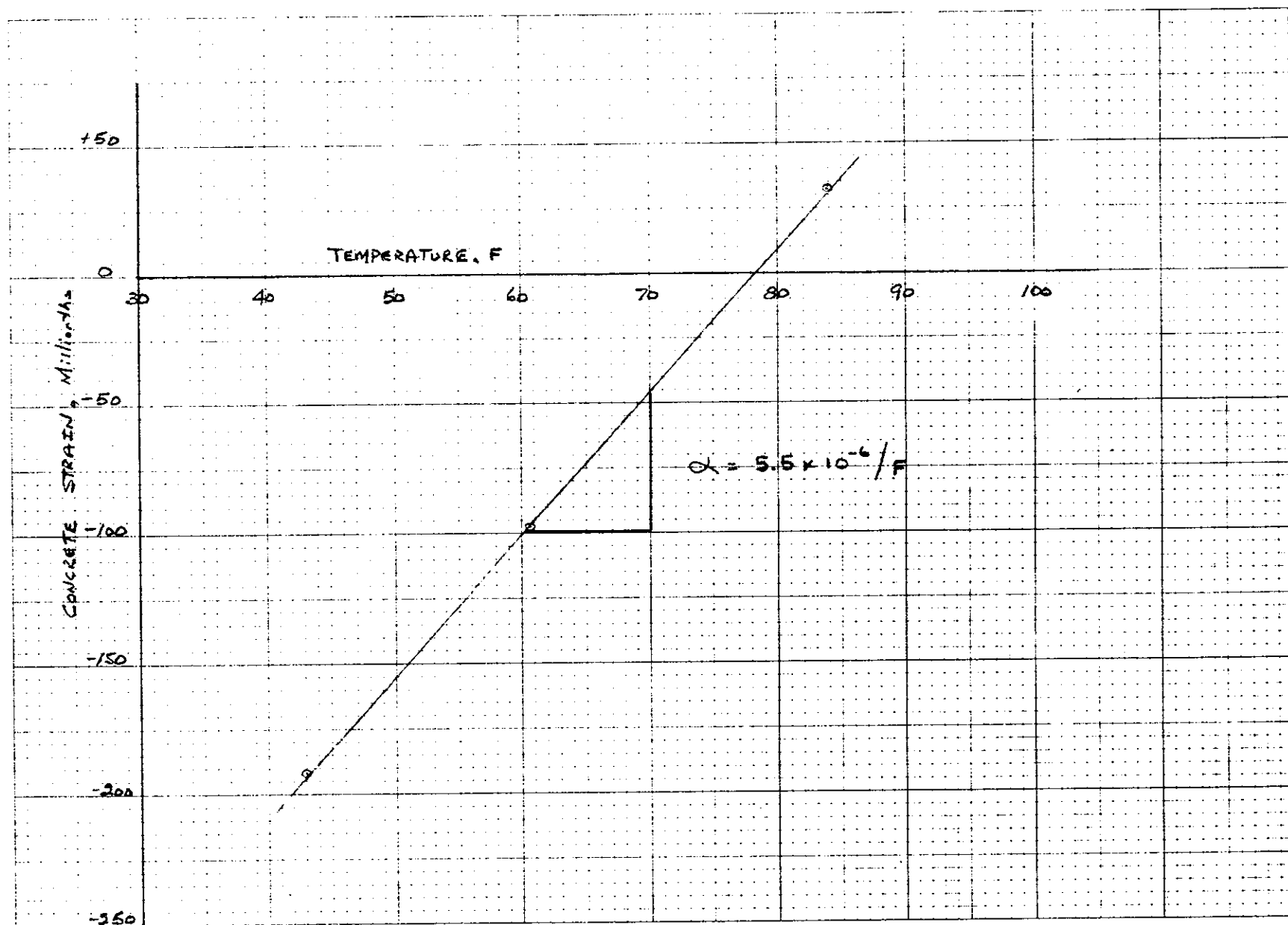


Fig. 4 Coefficient of Linear Thermal Expansion, Mixture PF

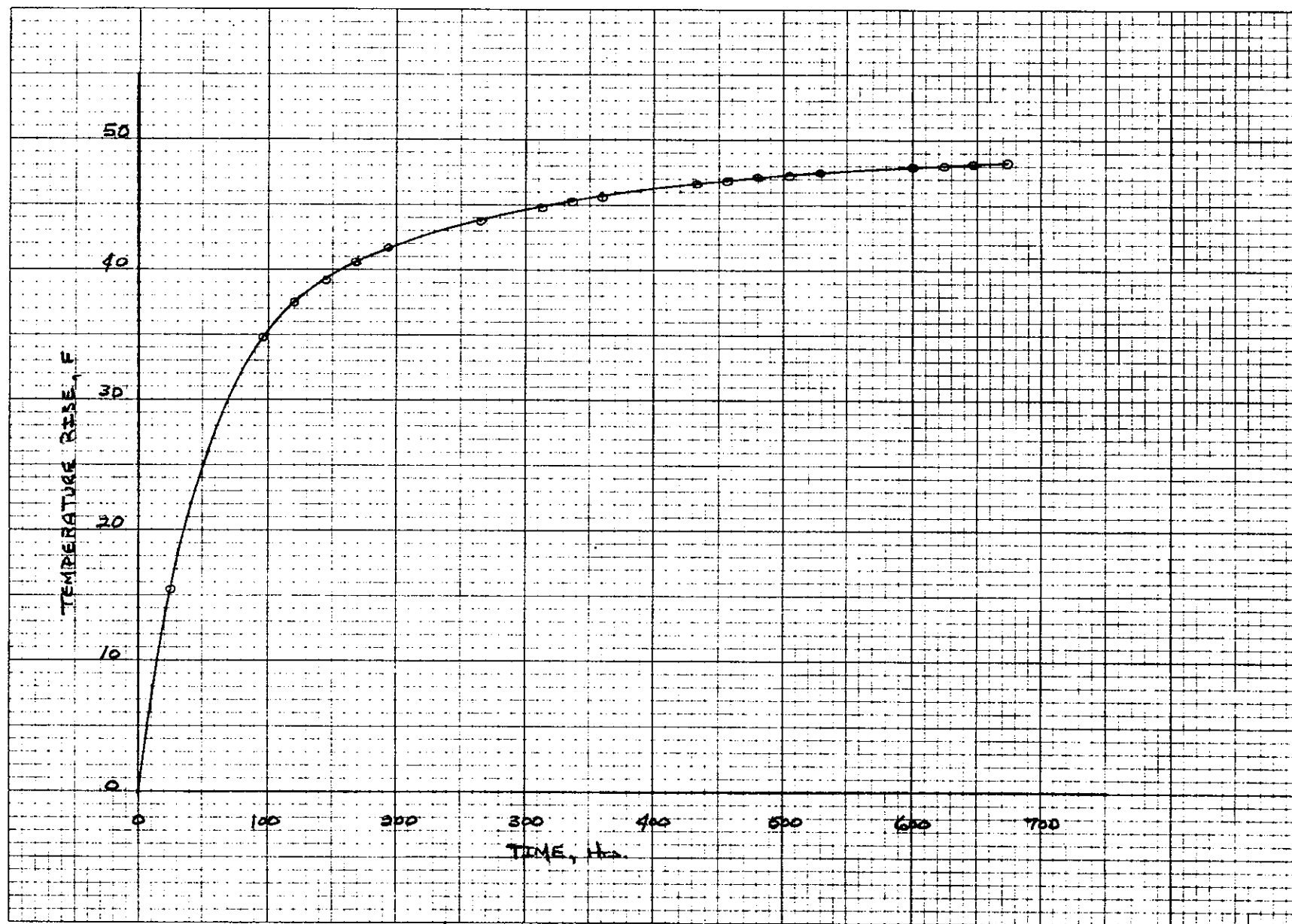


Fig. 5 Adiabatic Temperature Rise, Mixture 7

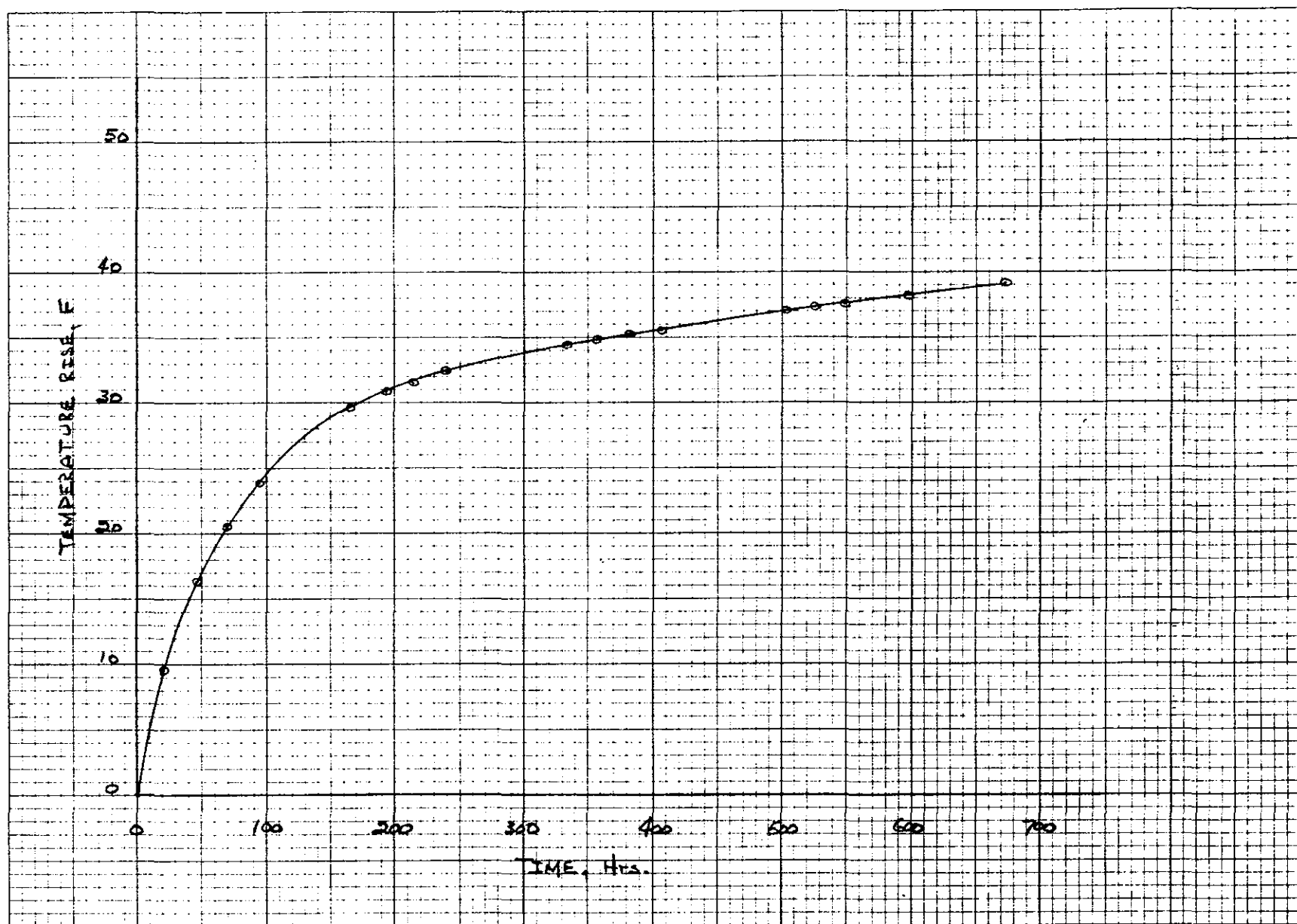


Fig. 6 Adiabatic Temperature Rise, Mixture 7F

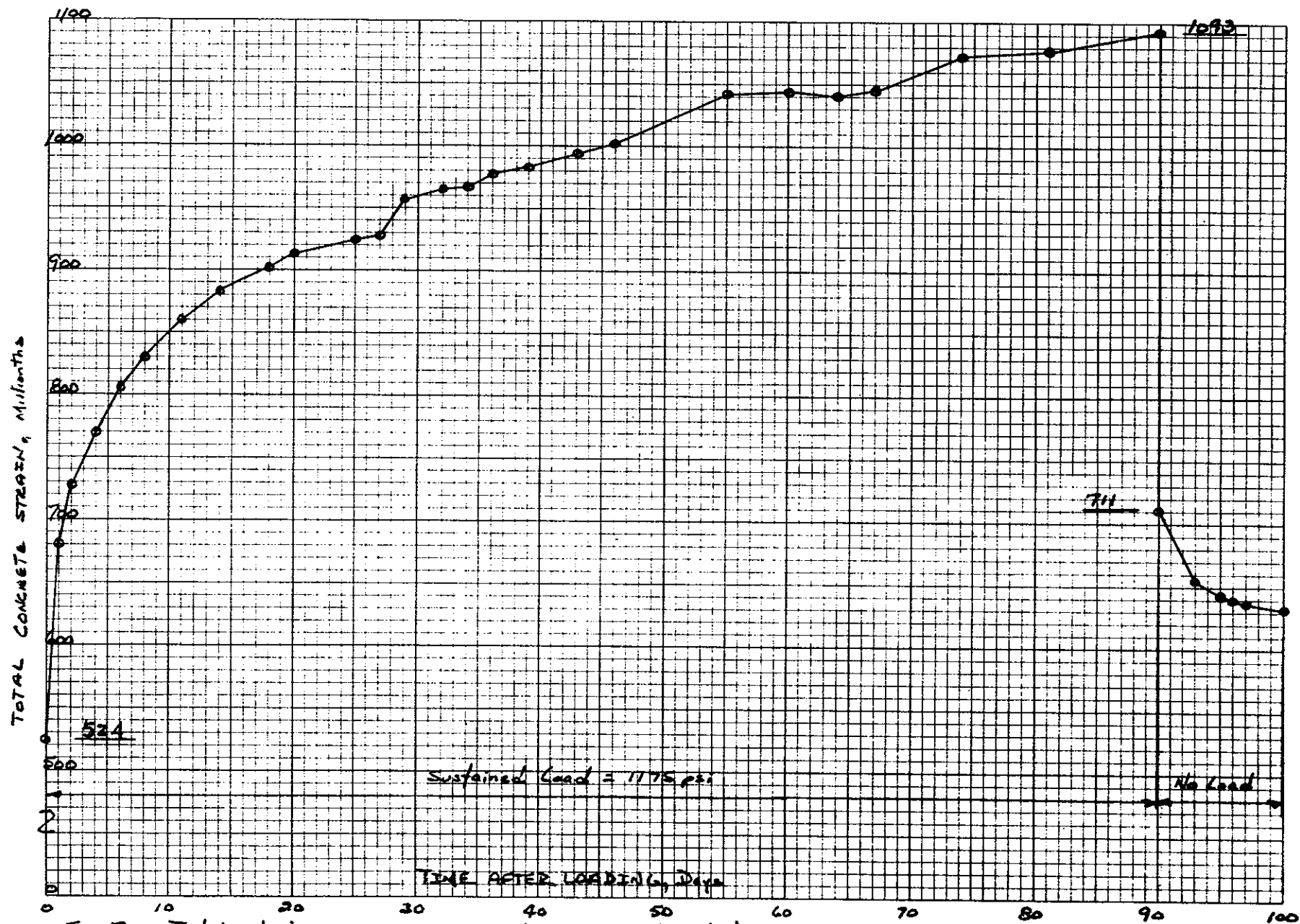


Fig. 7 Total strain Curve For Uniaxial Creep Test, Mixture P

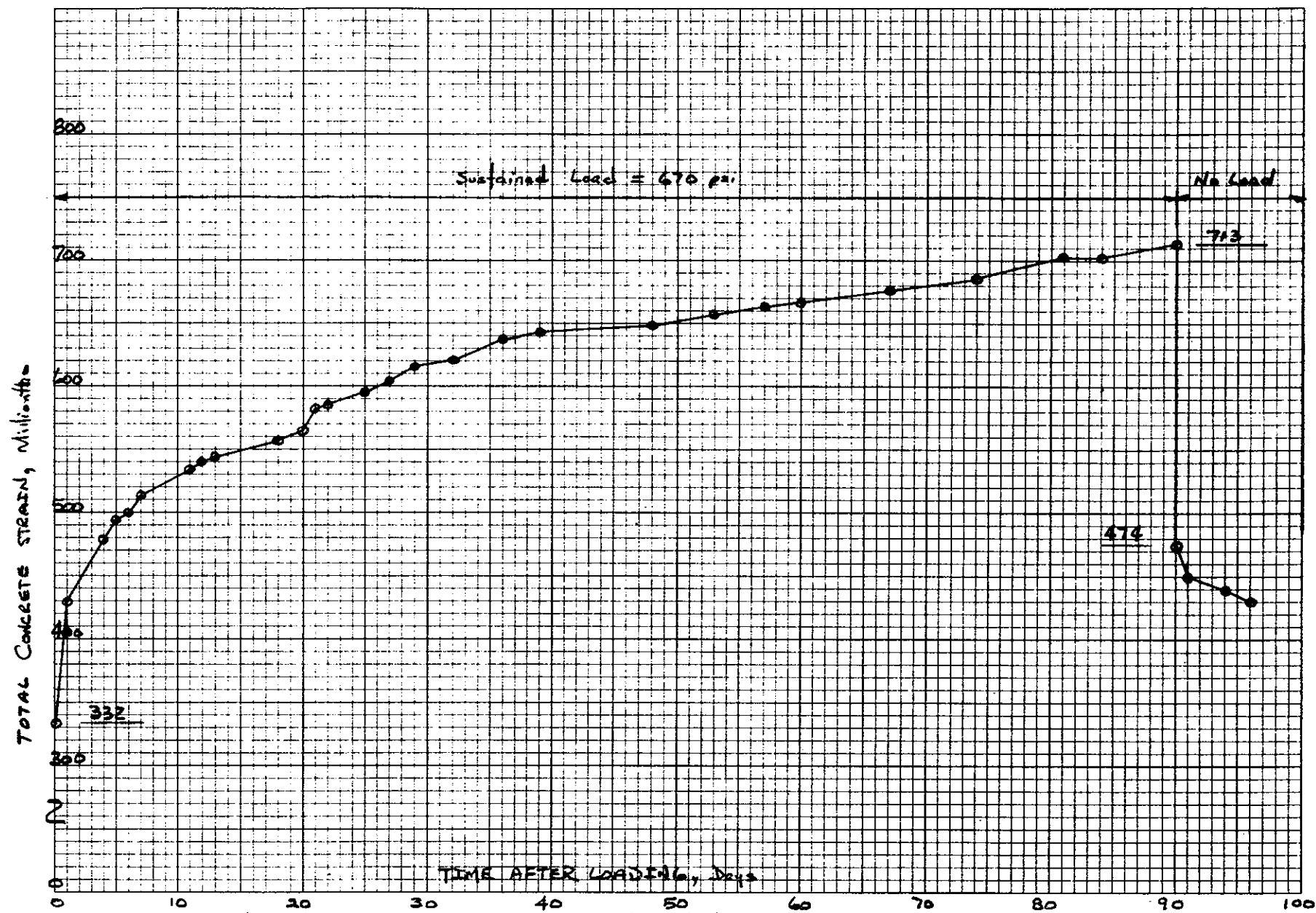


Fig. 8 Total Strain Curve For Uniaxial Creep Test, Mixture PF

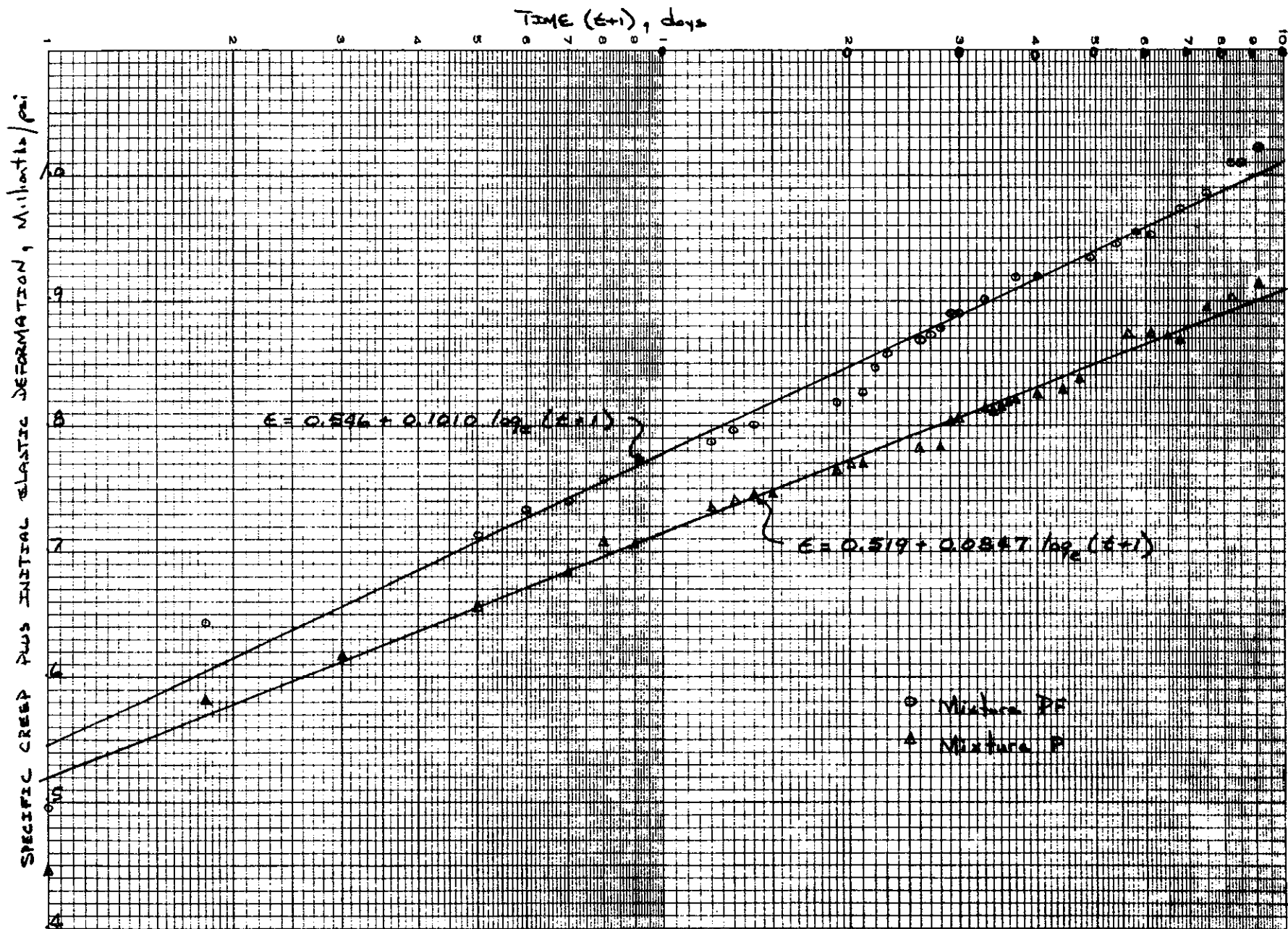


Fig. 9 Results of Uniaxial Creep Test

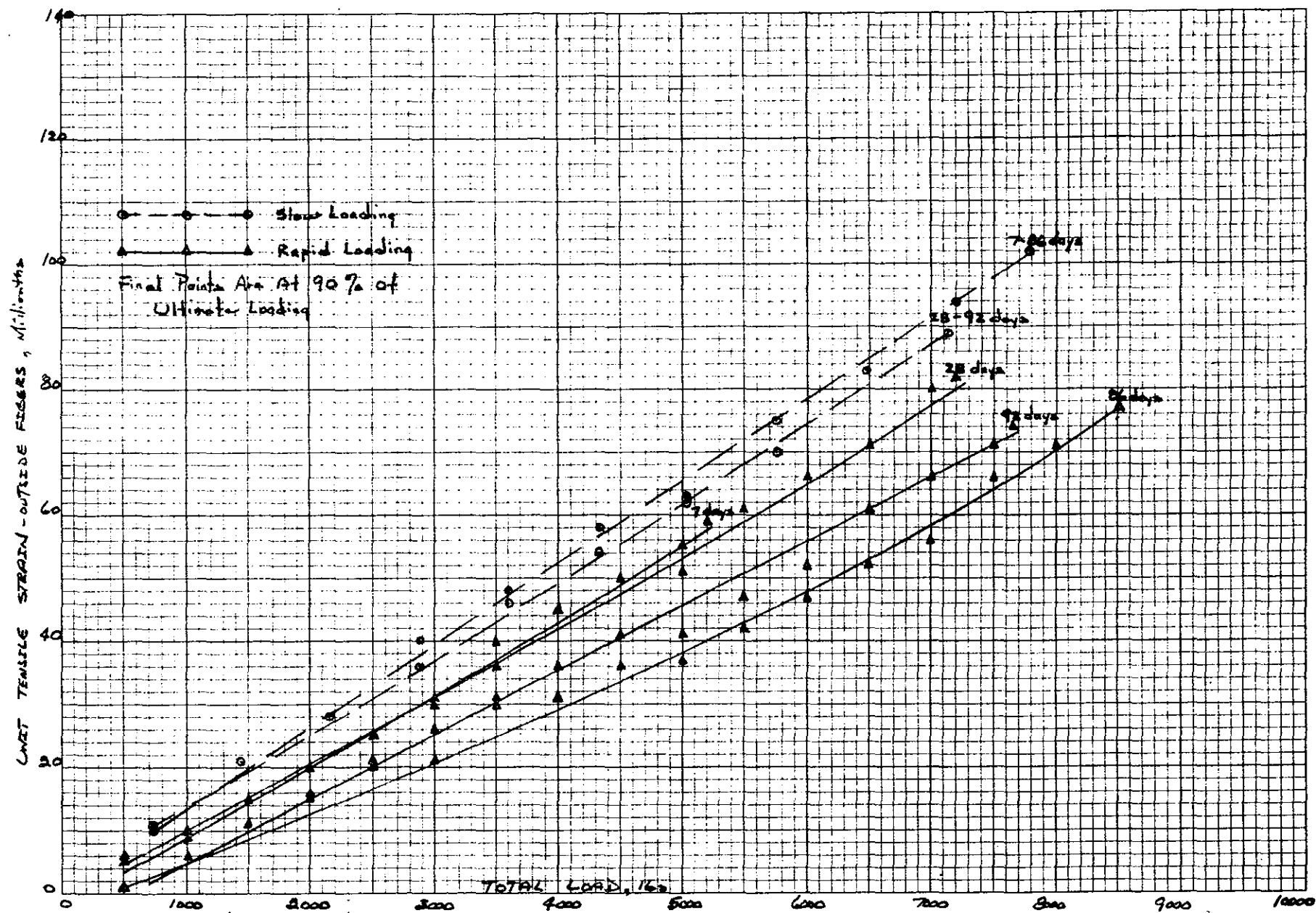


Fig. 10 Unit Tensile Strains, Mixture P, Round 1

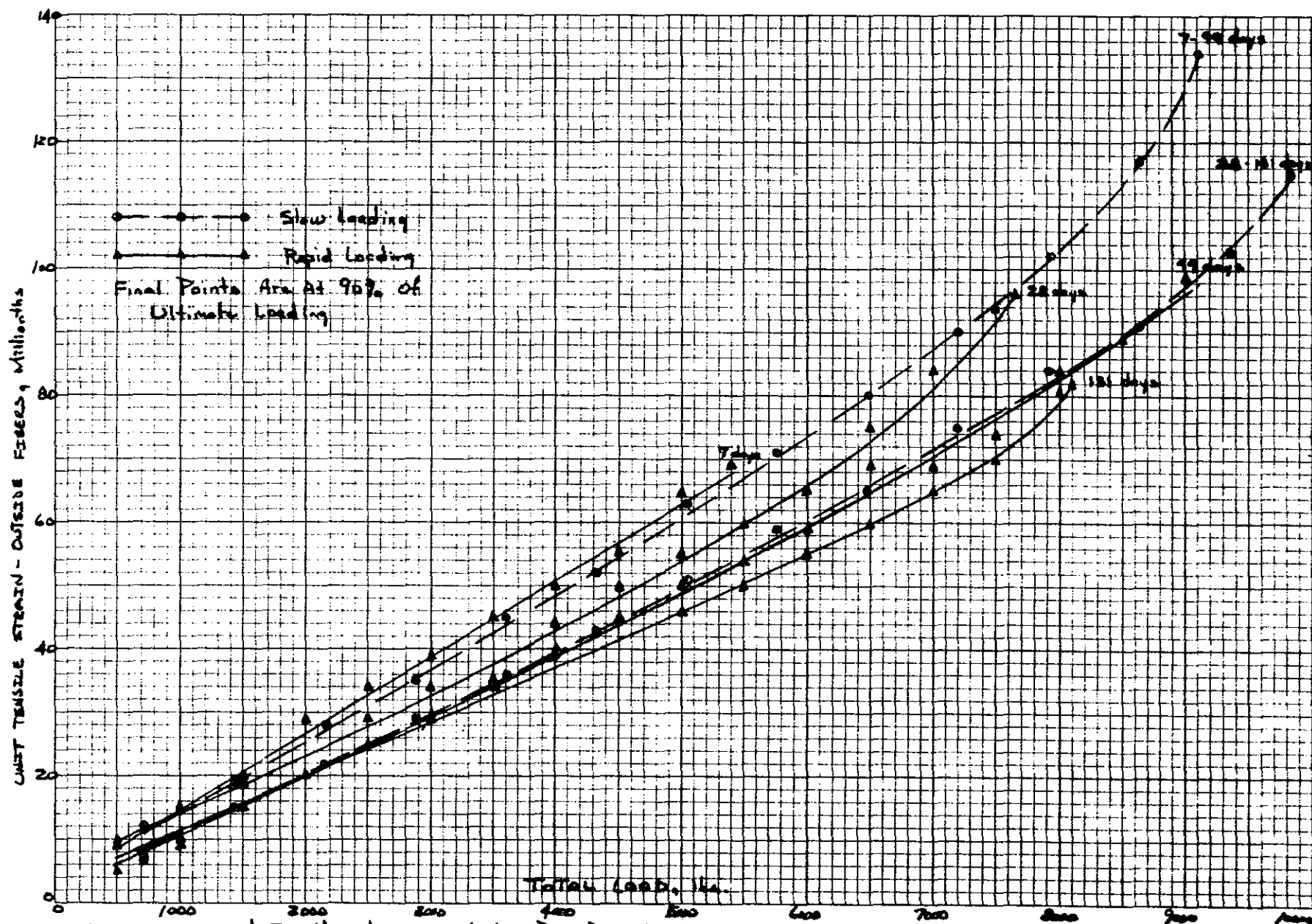


Fig. 14. Unit Tensile Strains, Mixture P, Round 2

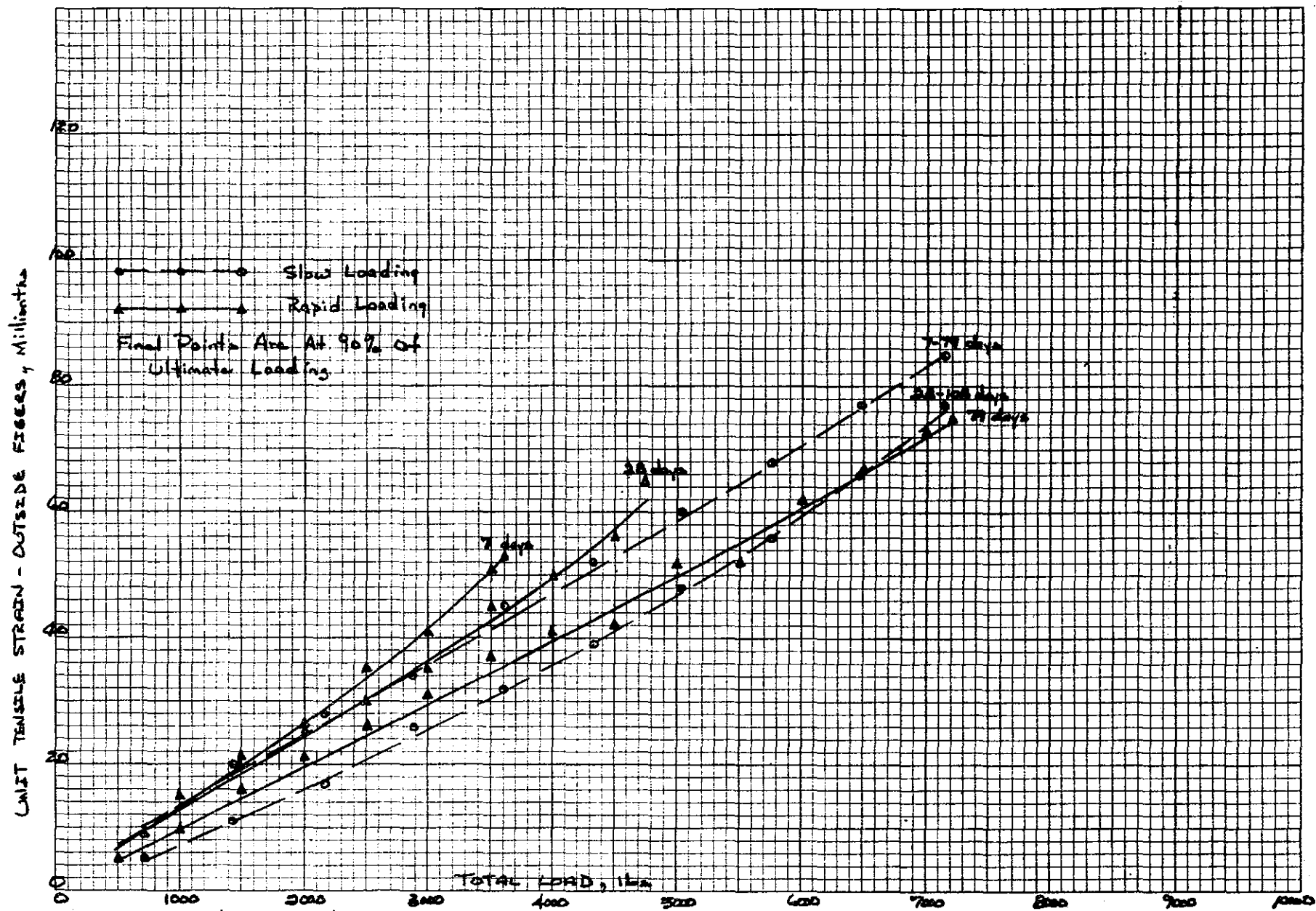


Fig. 12. Unit Tensile strain, Mixture PF, Round 1

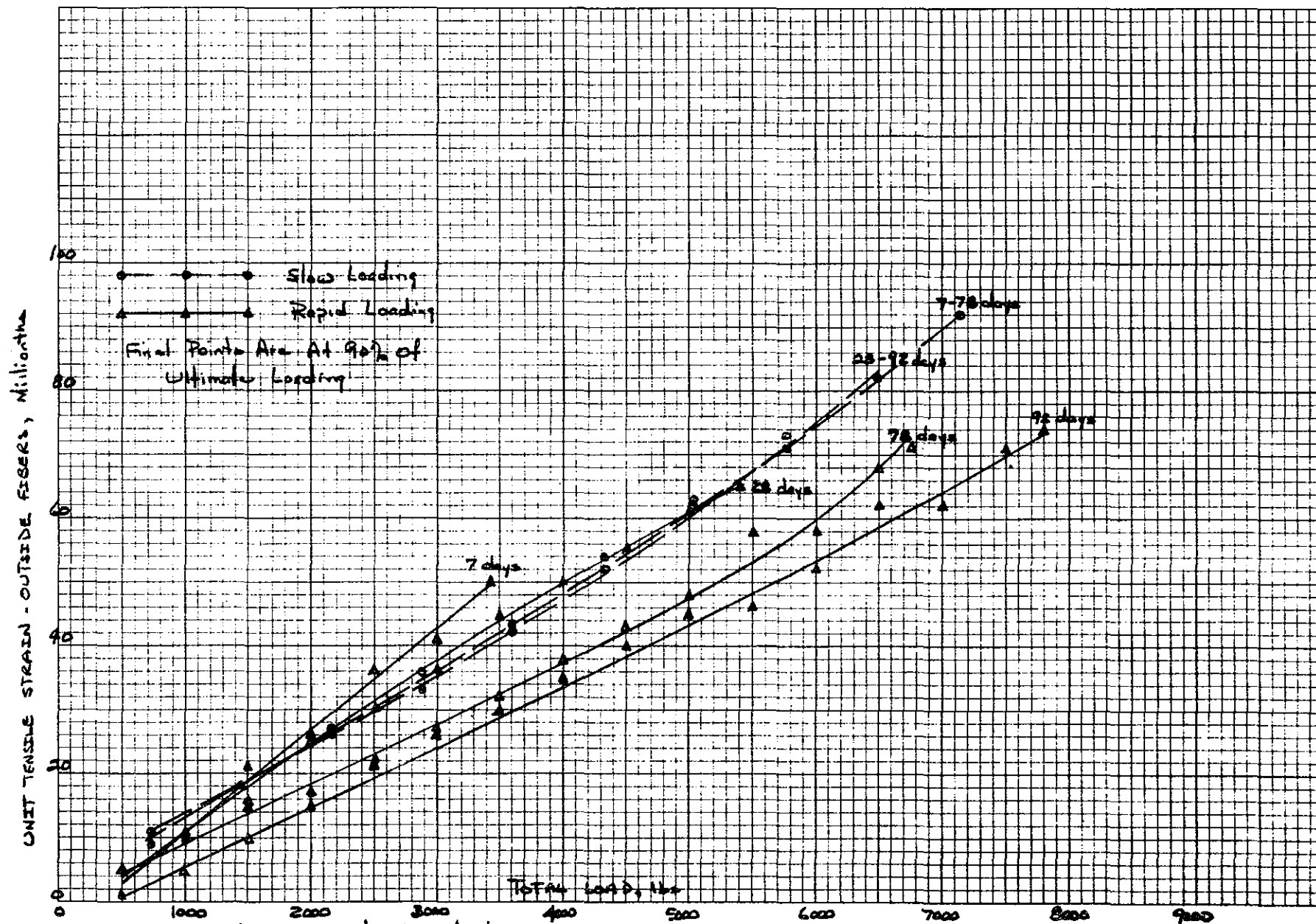


Fig. 13. Unit Tensile Strain, Mixture PF, Round 2

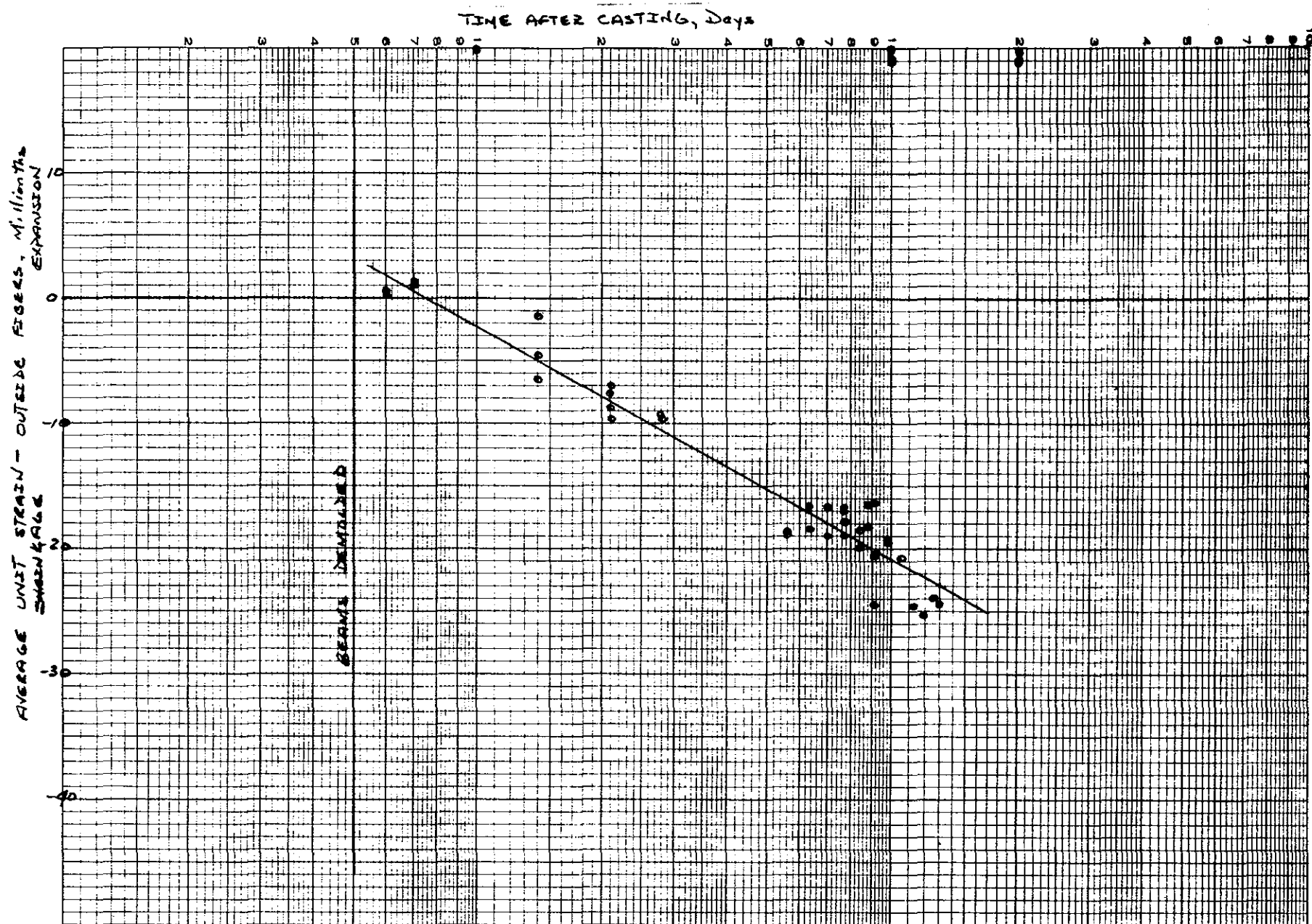


Fig. 14 Autogenous Length change of Beams in Storage. Mixture P

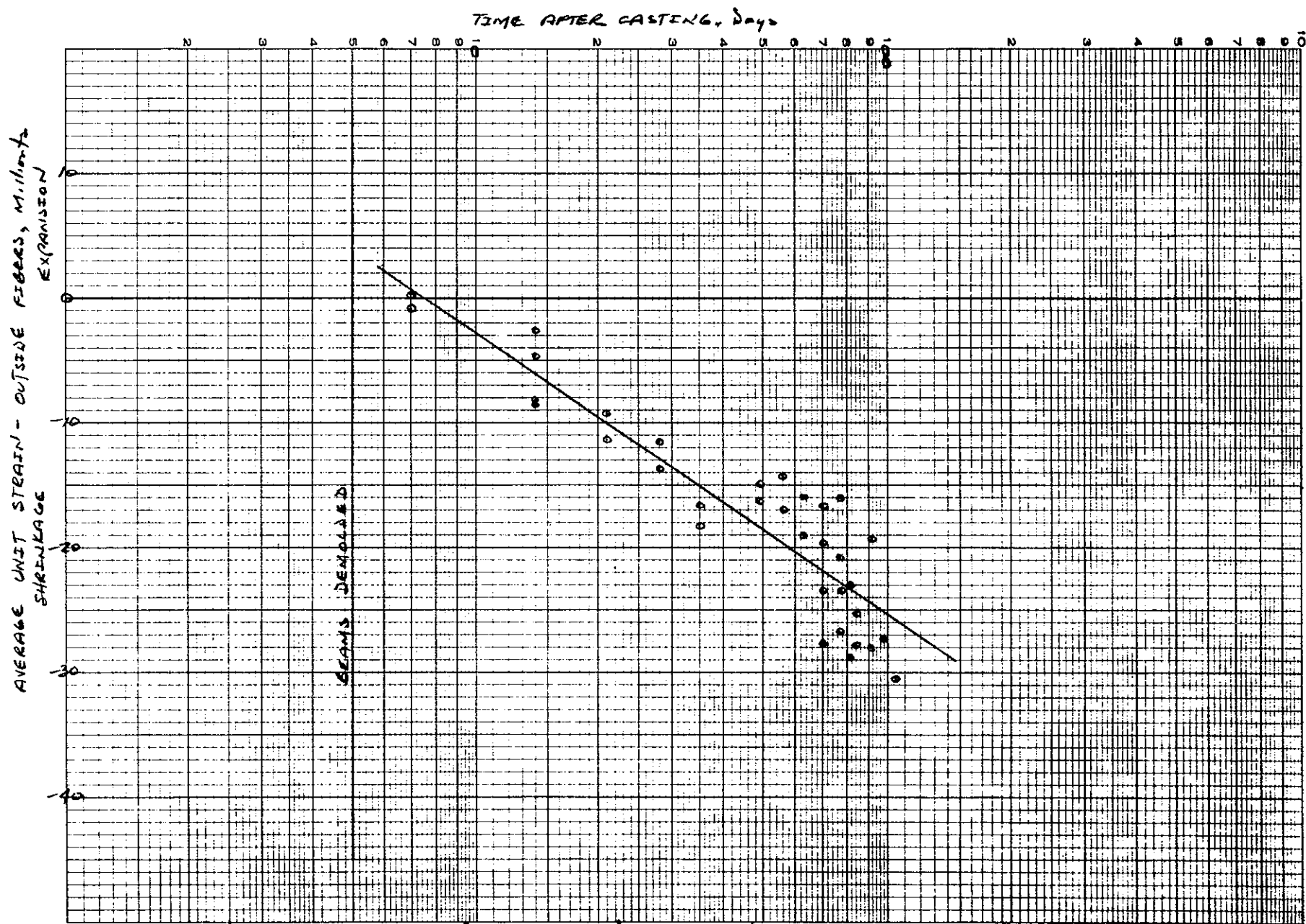


Fig. 15. Autogenous Length Change of Beams in Storage, Mixture 2F.

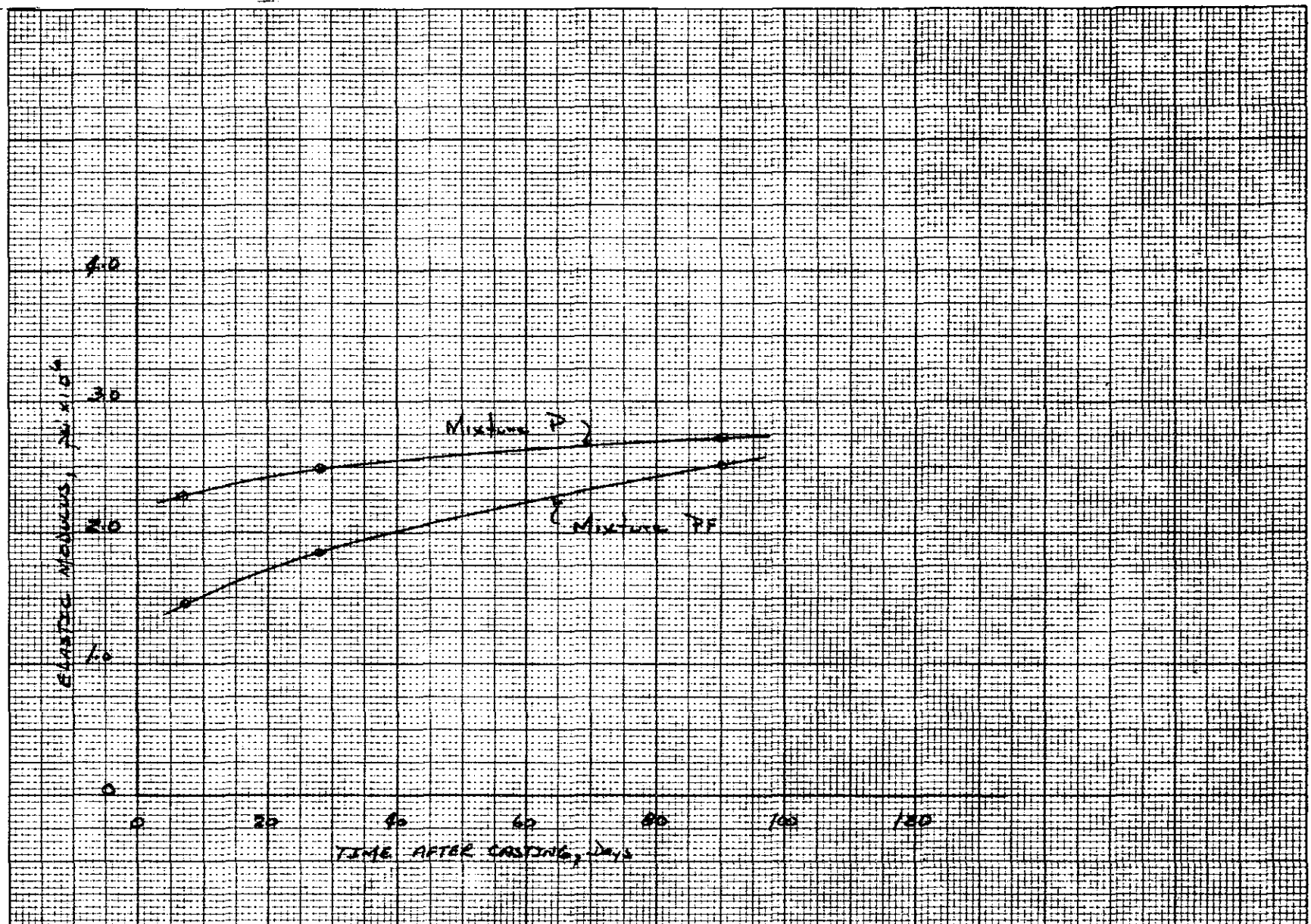


Fig 16. Variation in Elastic Modulus with Time

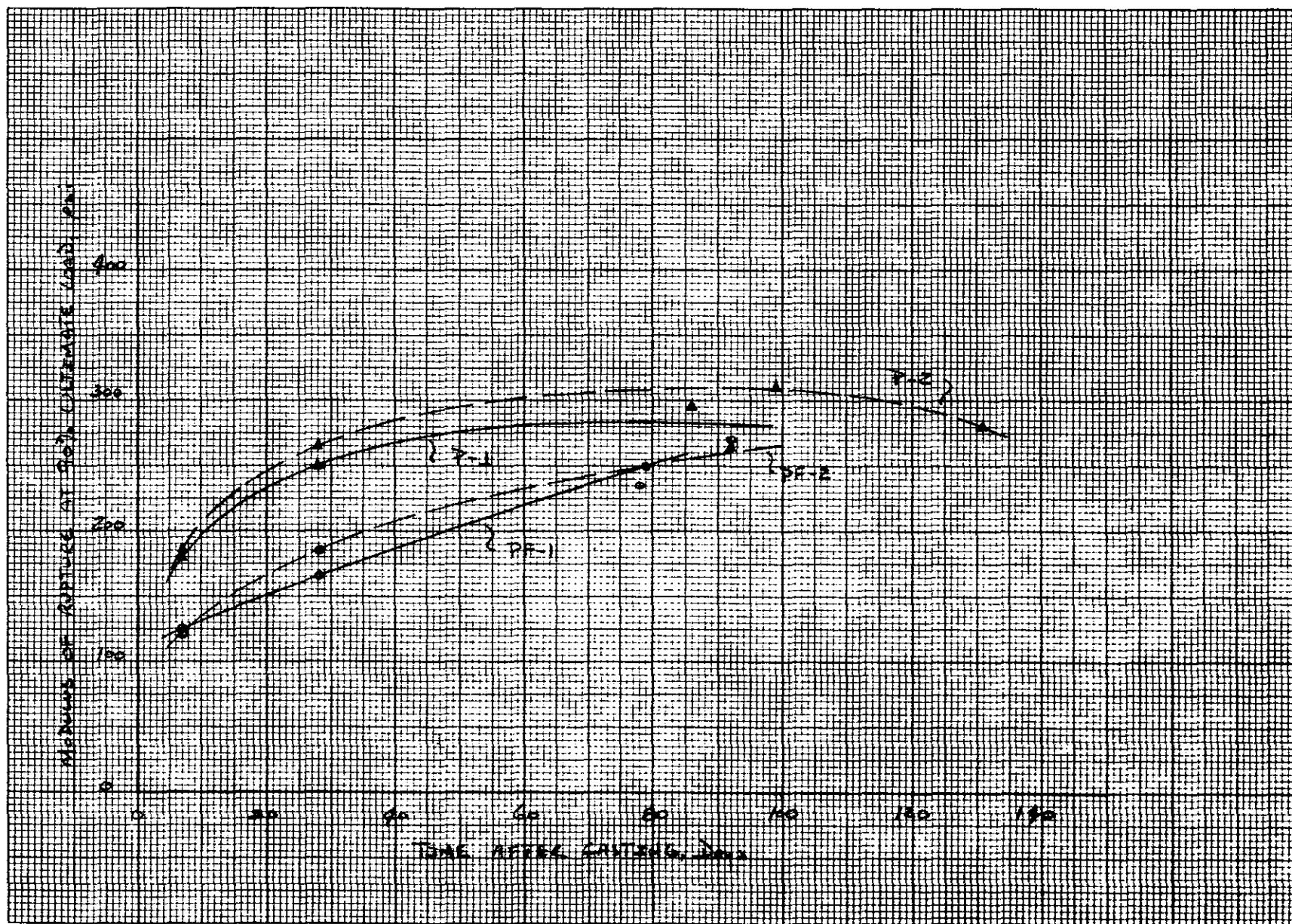


Fig. 17 Modulus of Rupture Determined From Rapid-Load Tests.

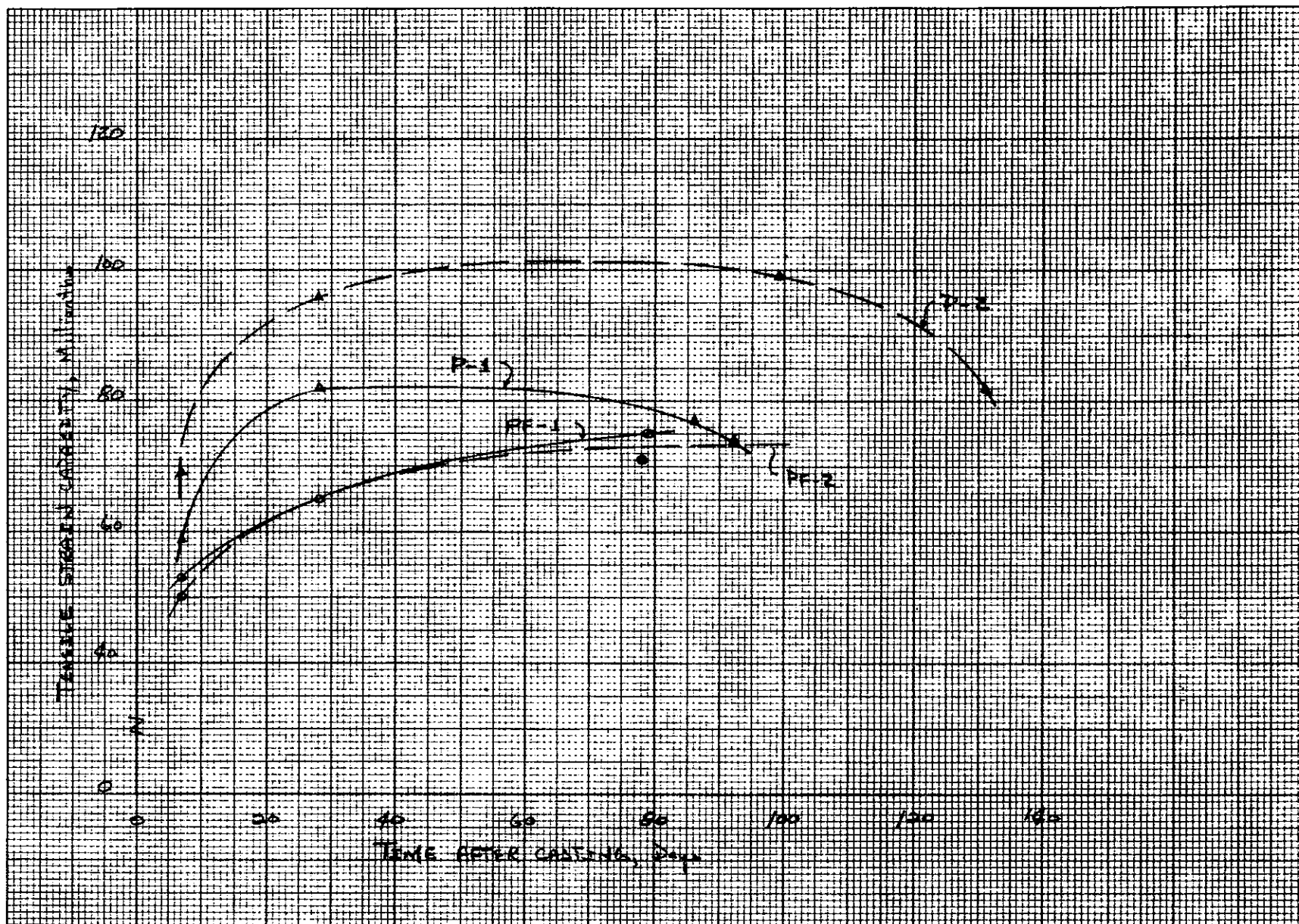


Fig. 1B Tensile Strain Capacity, Rapid Load Tests.

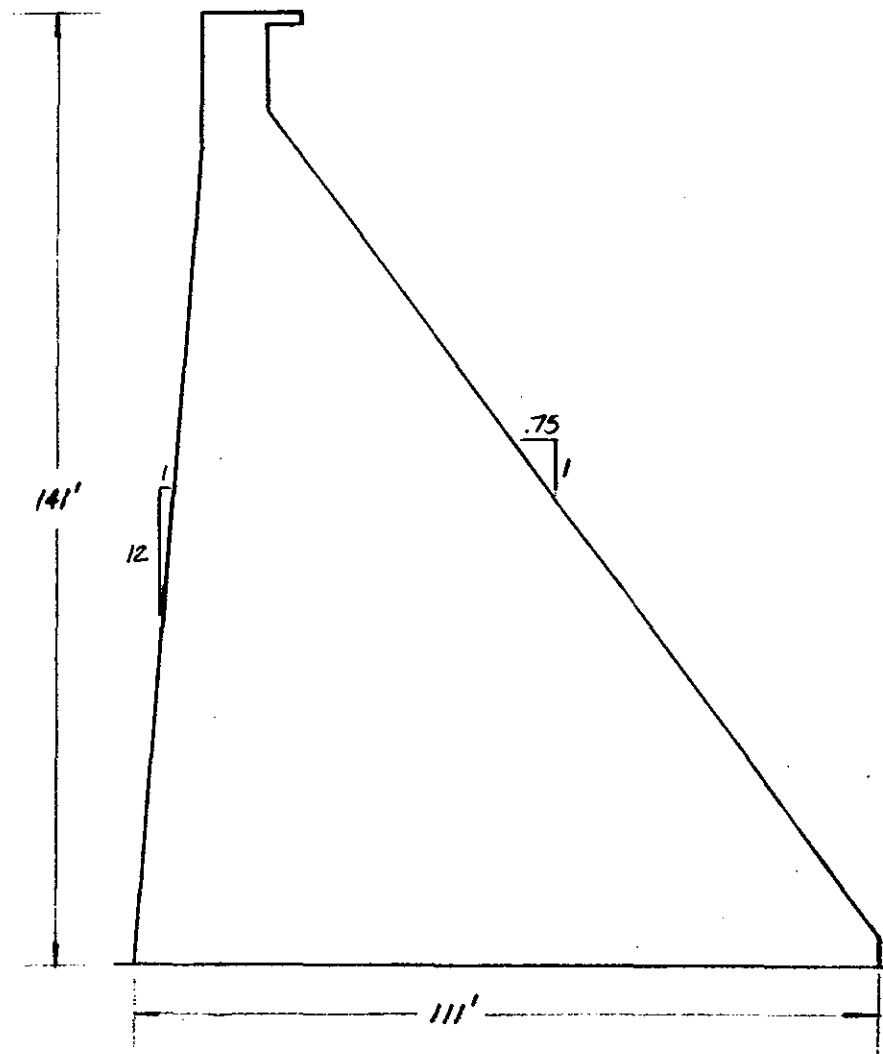


Fig. 19. Trumbull Pond Dam - Section at Station 3+20

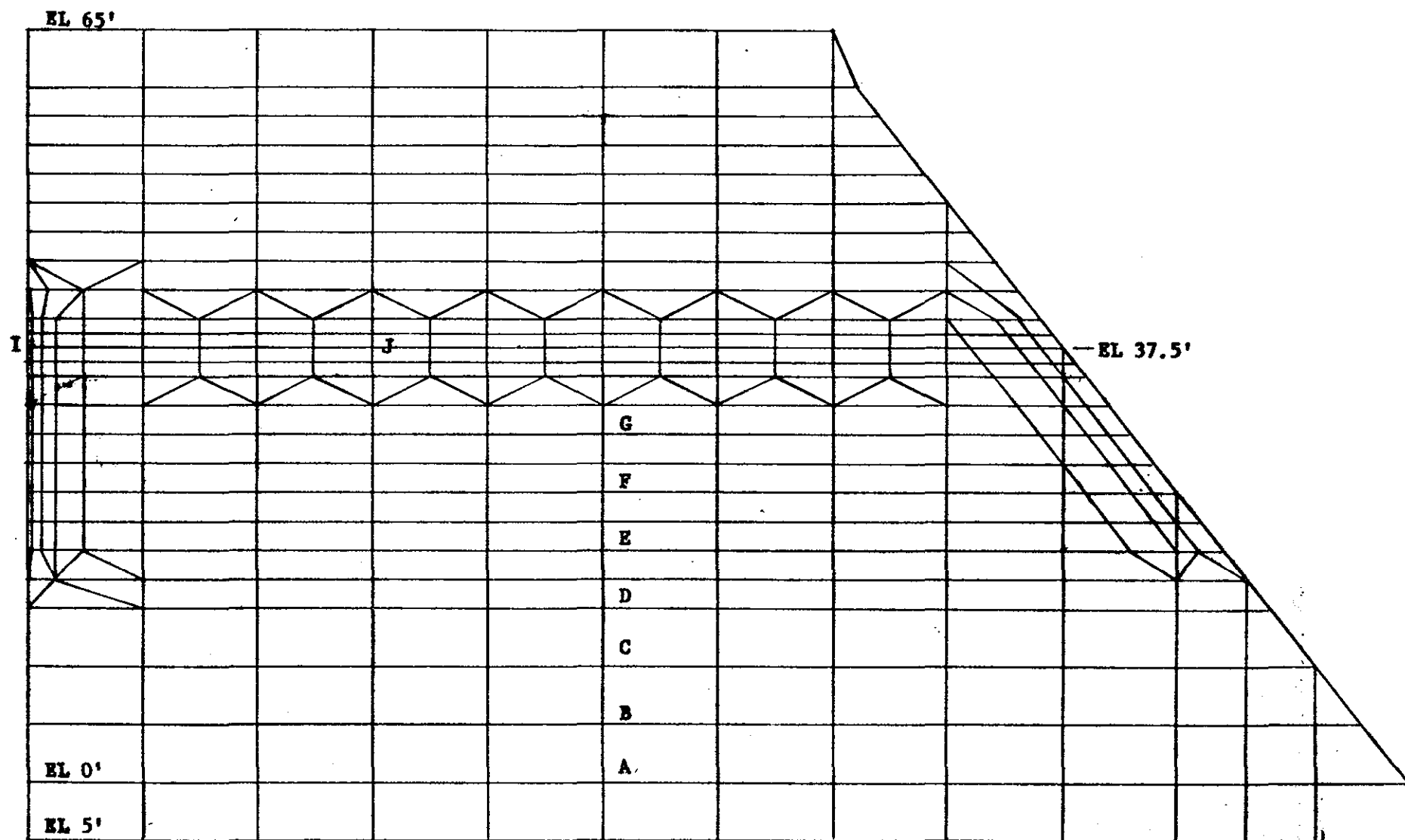


Fig. 20. Finite Element Model

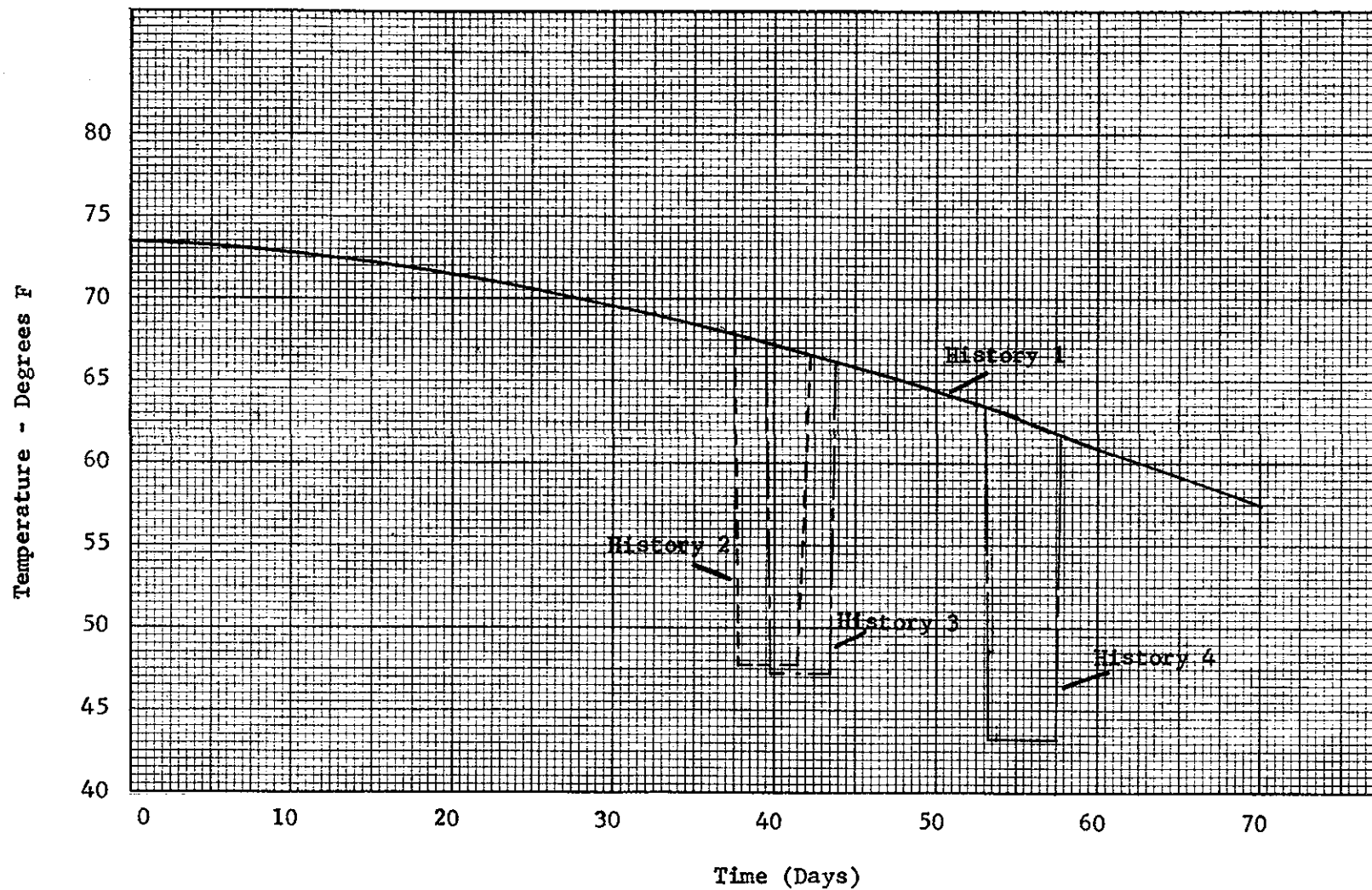


Fig. 21. Ambient Temperature Histories

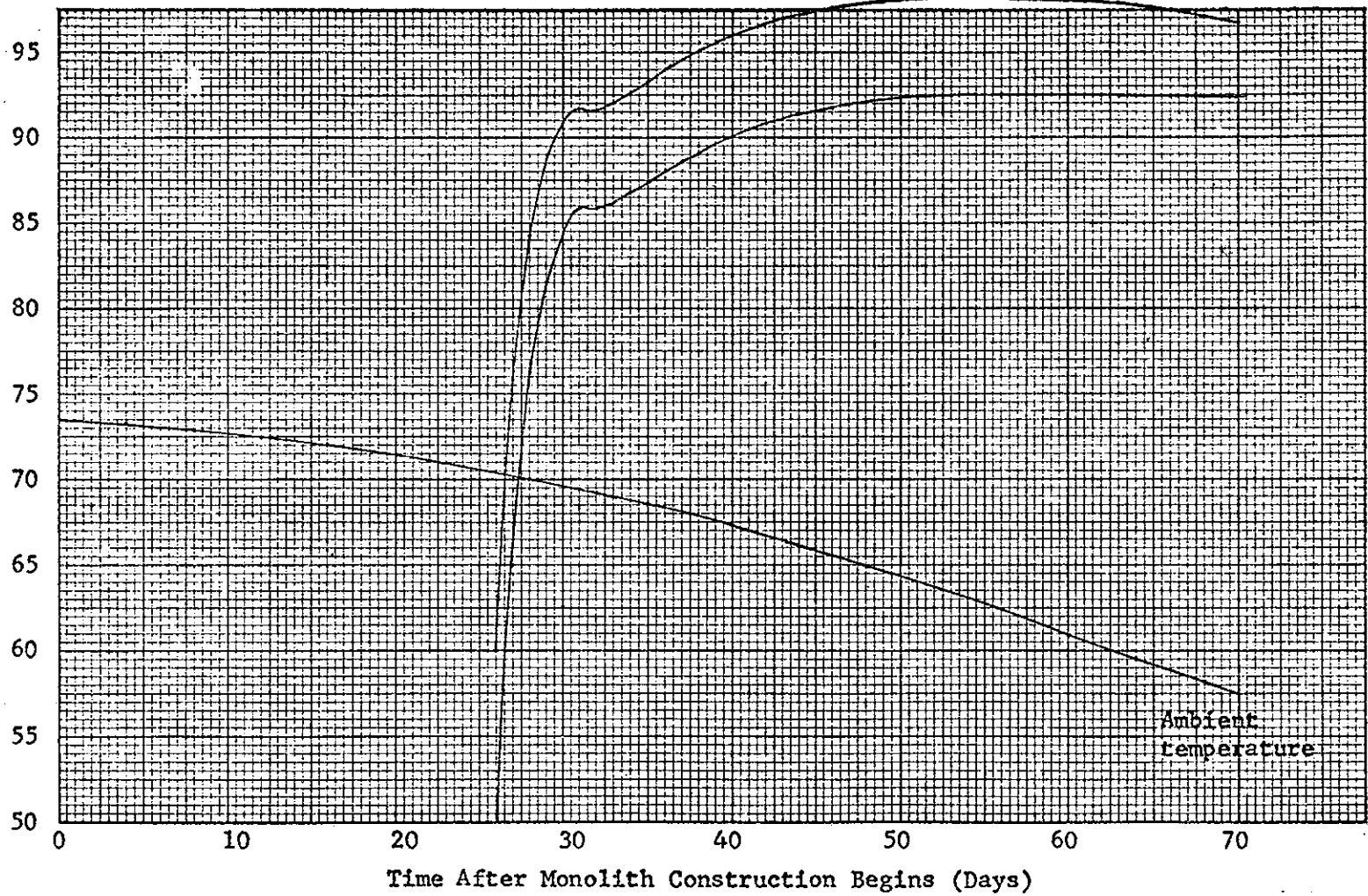


Fig. 22. Maximum Temperature Rise for Mixture P at 50- and 60-Deg Placement Temperatures for 5-ft Lift Construction

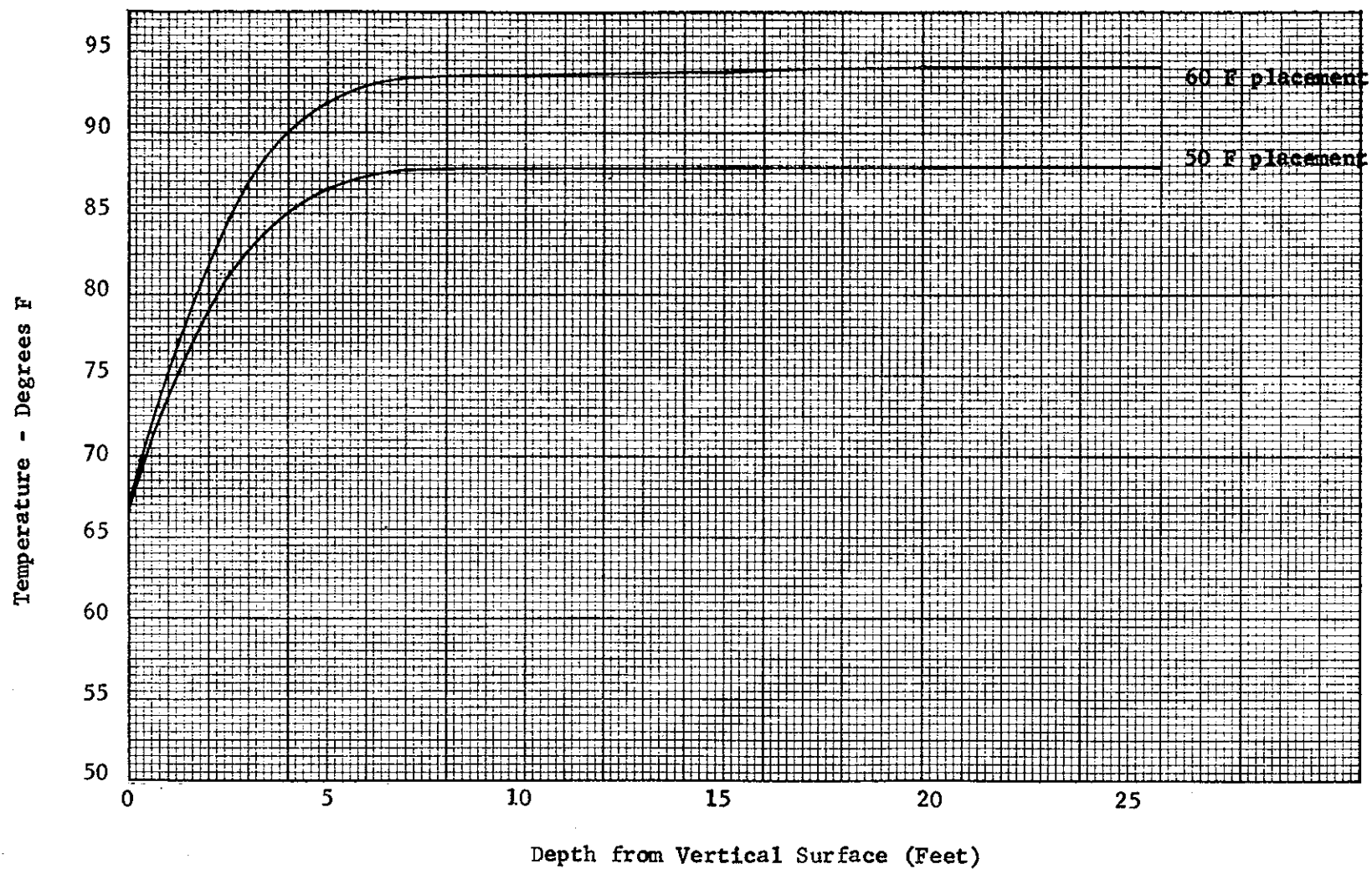


Fig. 23. Thermal Gradients for Concrete Placed at 50 and 60 F

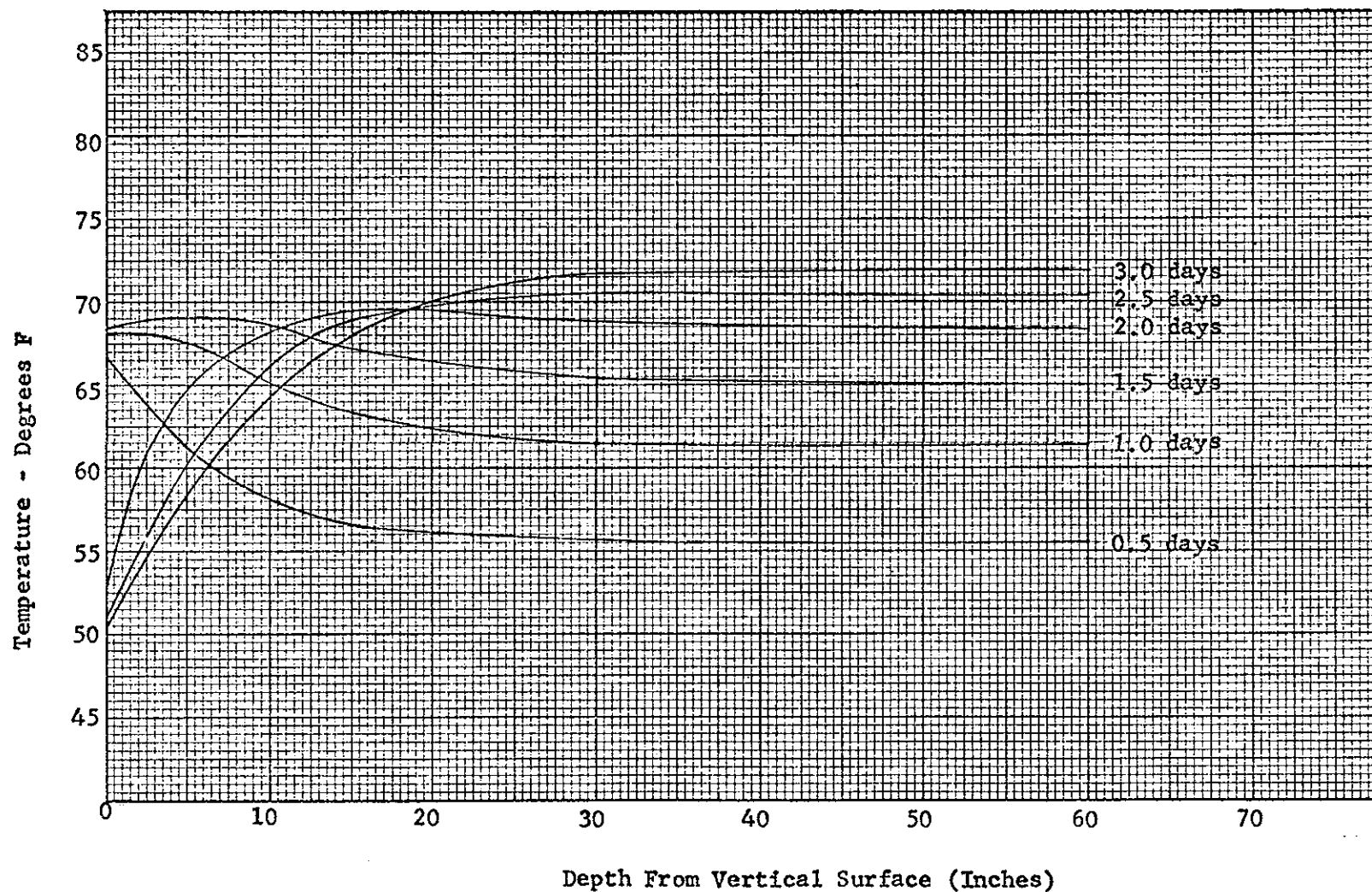


Fig. 24. Thermal Gradients - Effect of 20 Deg Ambient Temperature Drop at 1.5 Days After Lift Placement With No Insulation (1.0μ)

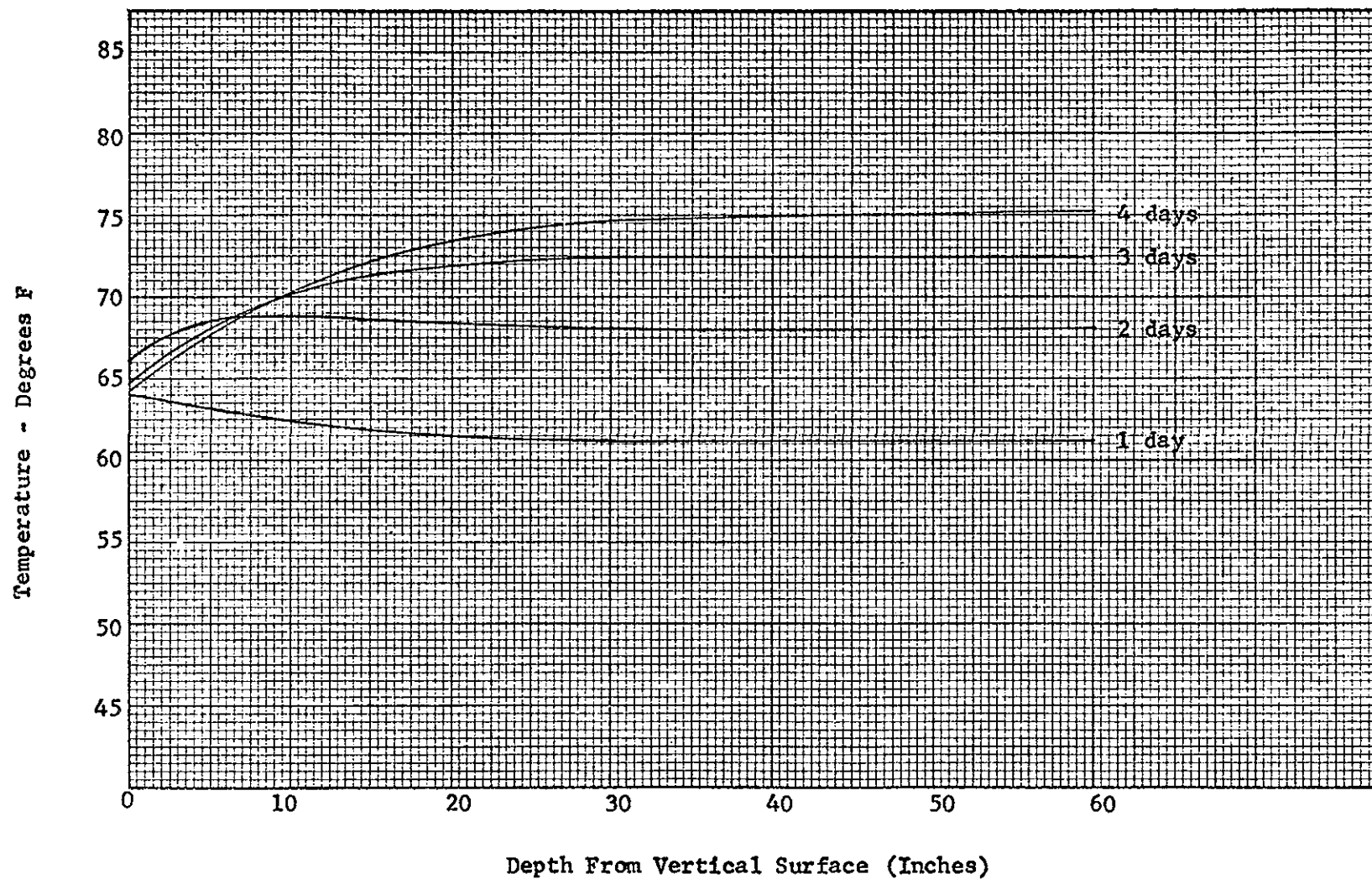
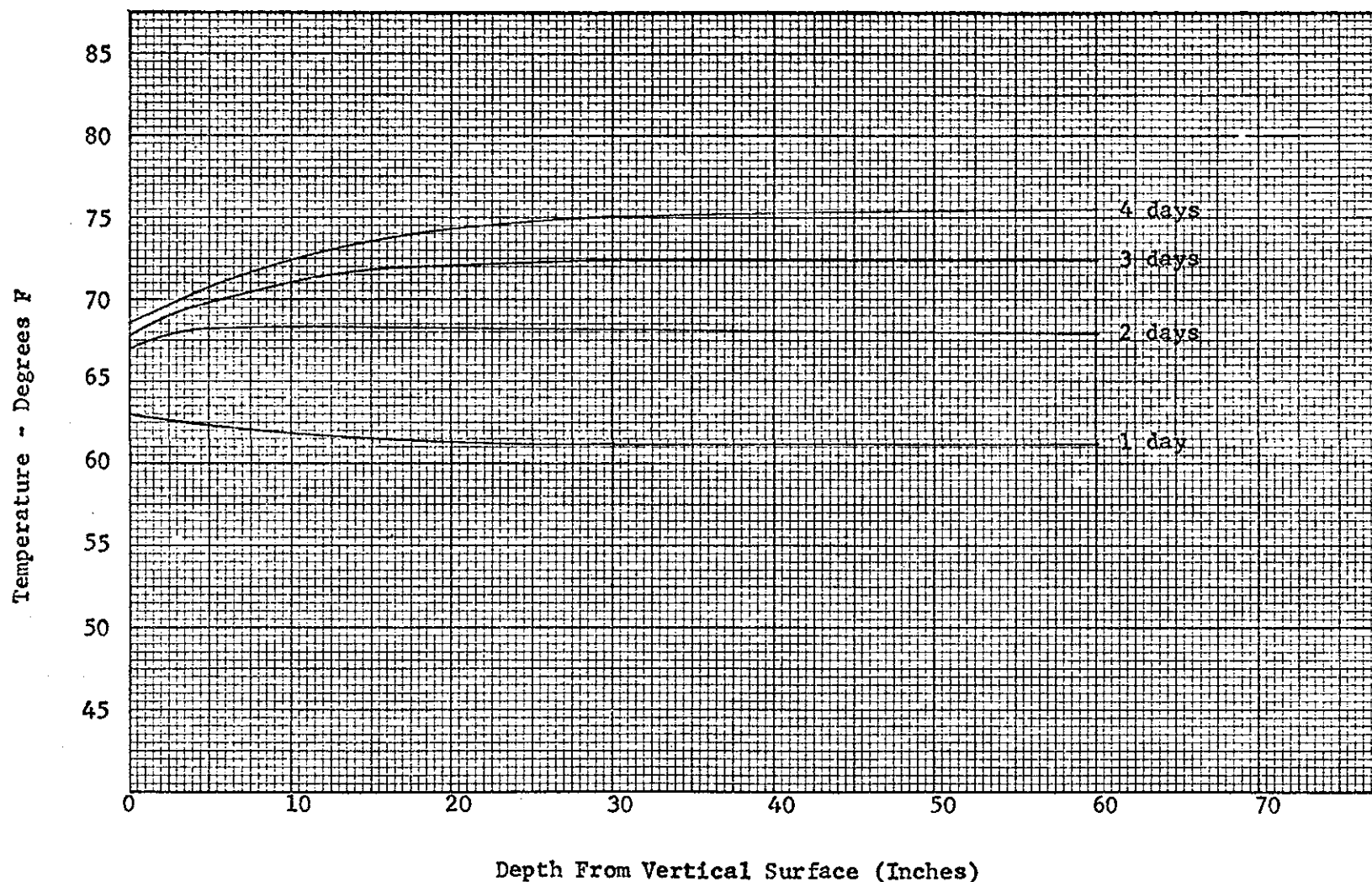


Fig. 25. Thermal Gradients-Effect of 20-Deg Ambient Temperature Drop at 1.50 Days After Lift Placement With 0.50 μ Insulation



Depth From Vertical Surface (Inches)
Fig. 26. Thermal Gradients-Effect of 20-Deg Ambient Temperature Drop
at 1.50 Days After Lift Placement With 0.25 μ Insulation

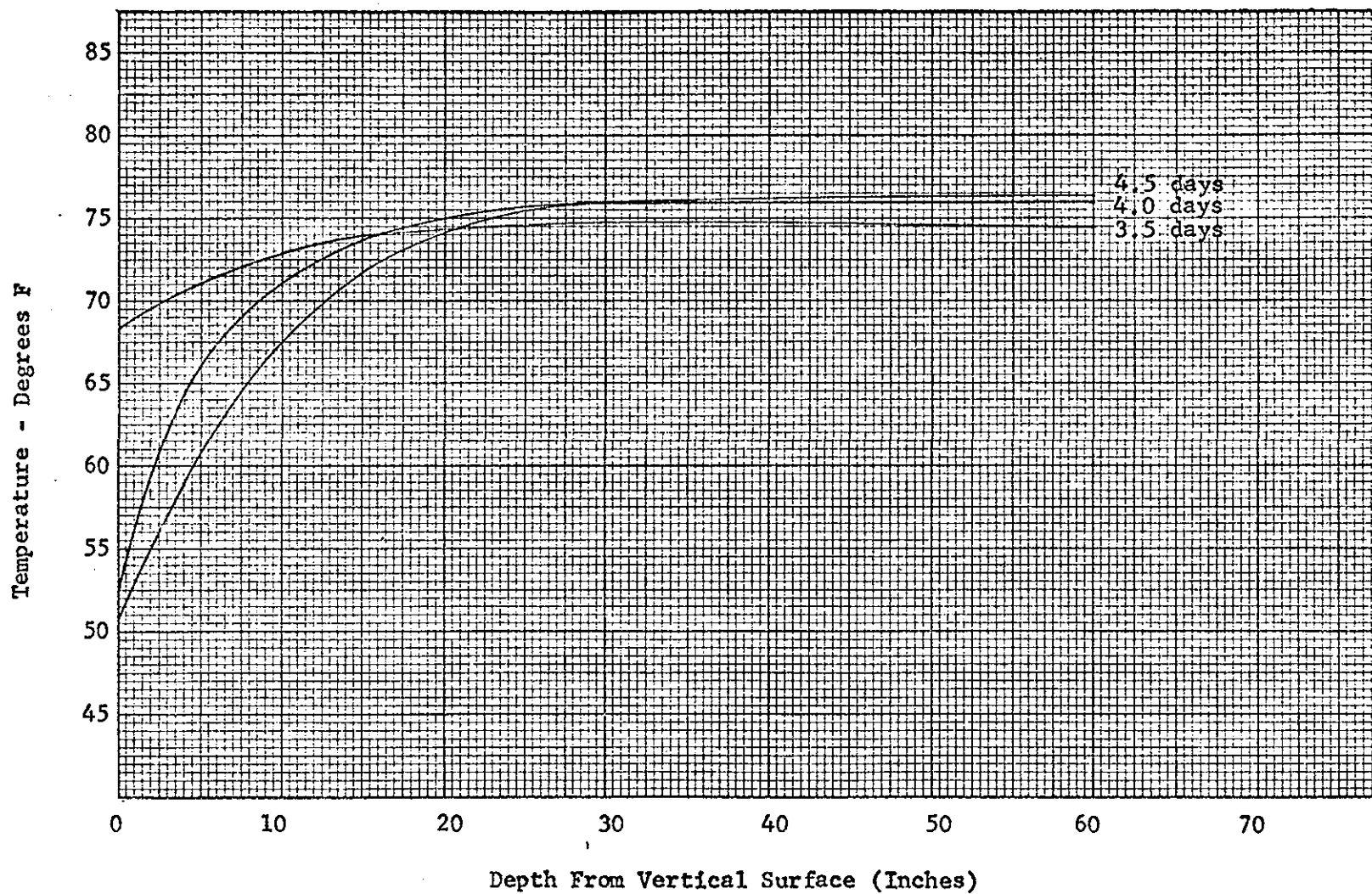


Fig.27. Thermal Gradients-Effect of 20-Deg Ambient Temperature Drop
at 3.5 Days After Lift Placement with No Insulation (1.0 μ)

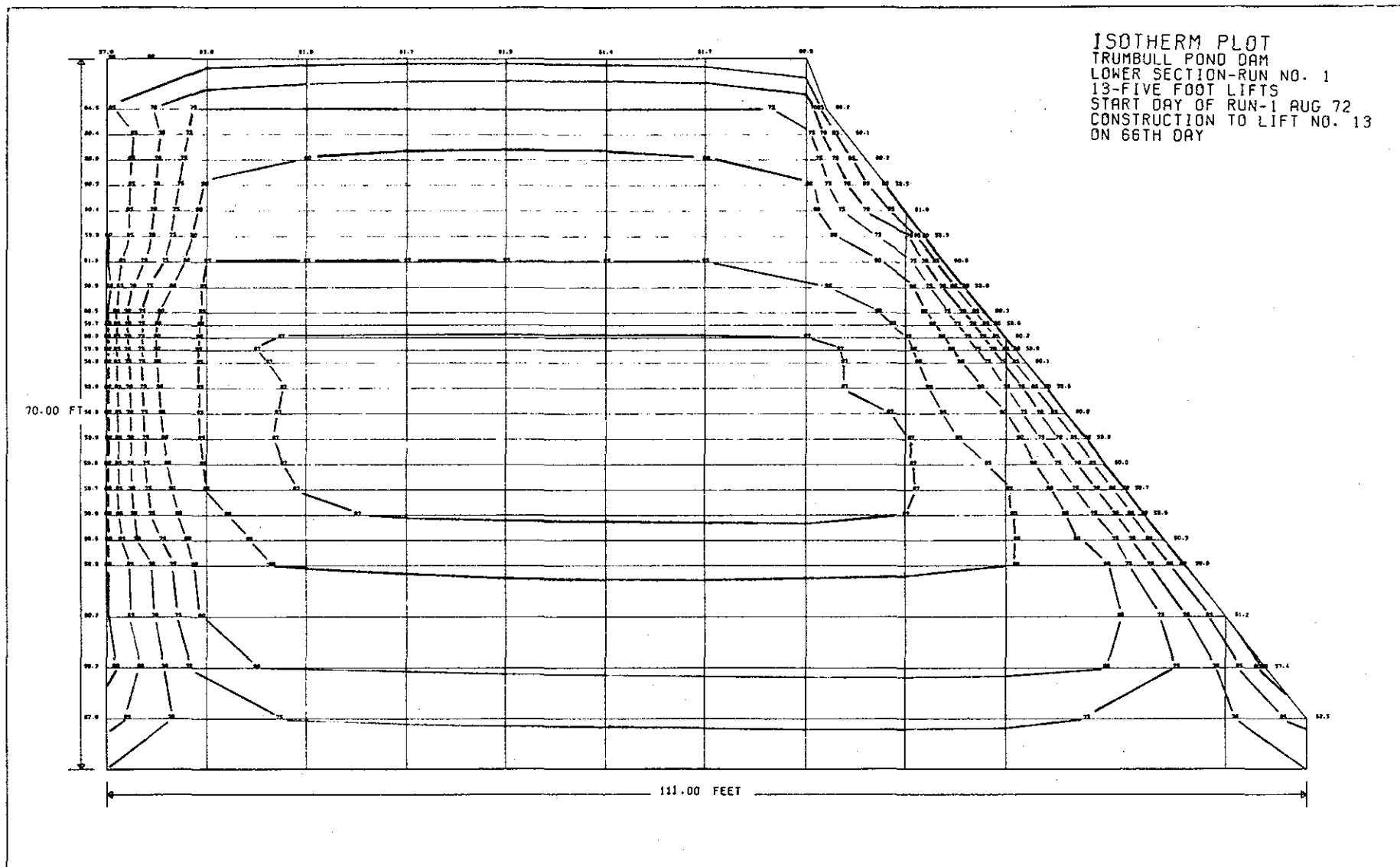
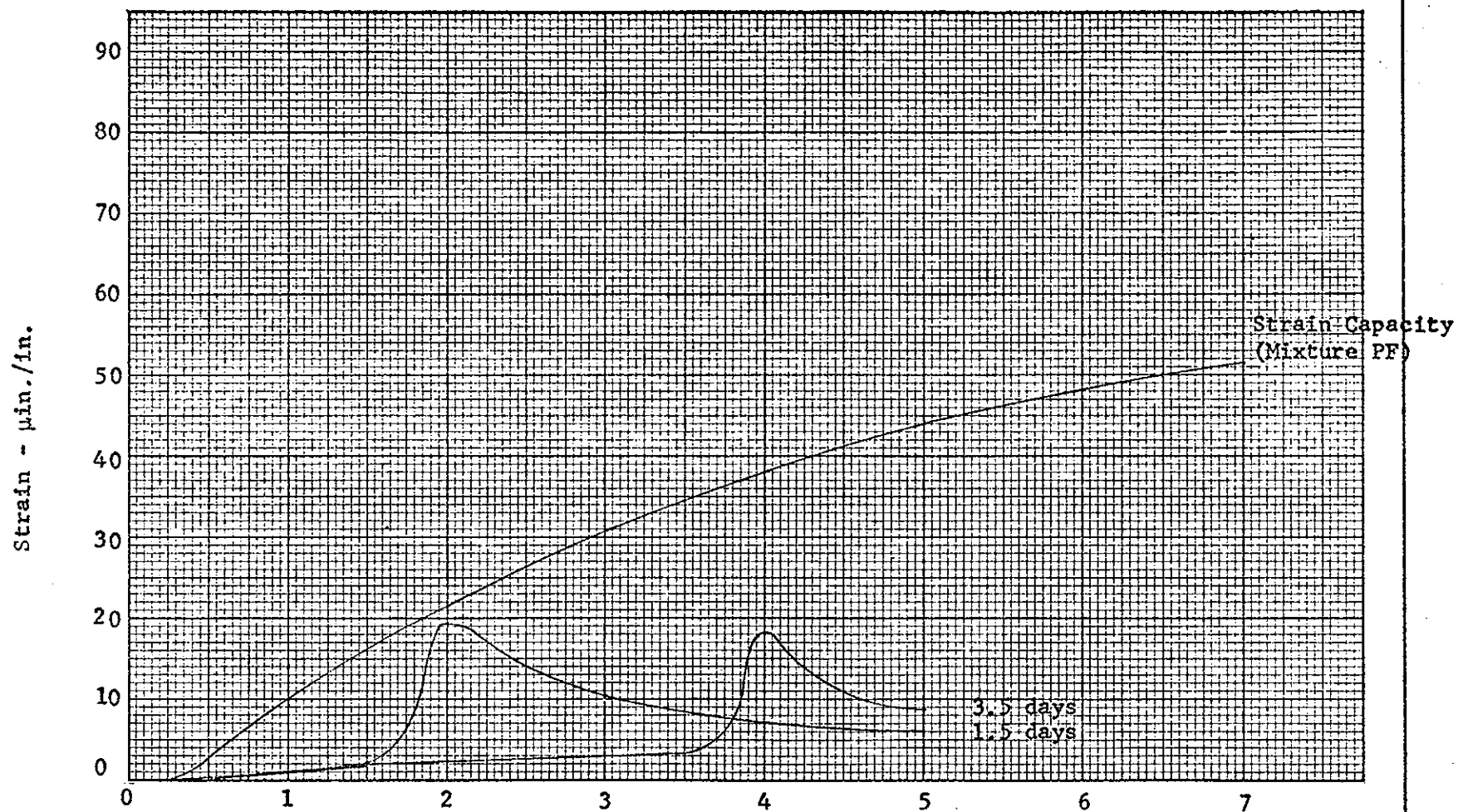


Fig. 28. Typical Isotherm Plot



Time After Lift Placement (Days)

Fig. 29. Thermally Induced Strain at 1.0 in. Depth for Ambient Temperature Drop at 1.5 and 3.5 Days After Placement--No Insulation (1.0 μ)

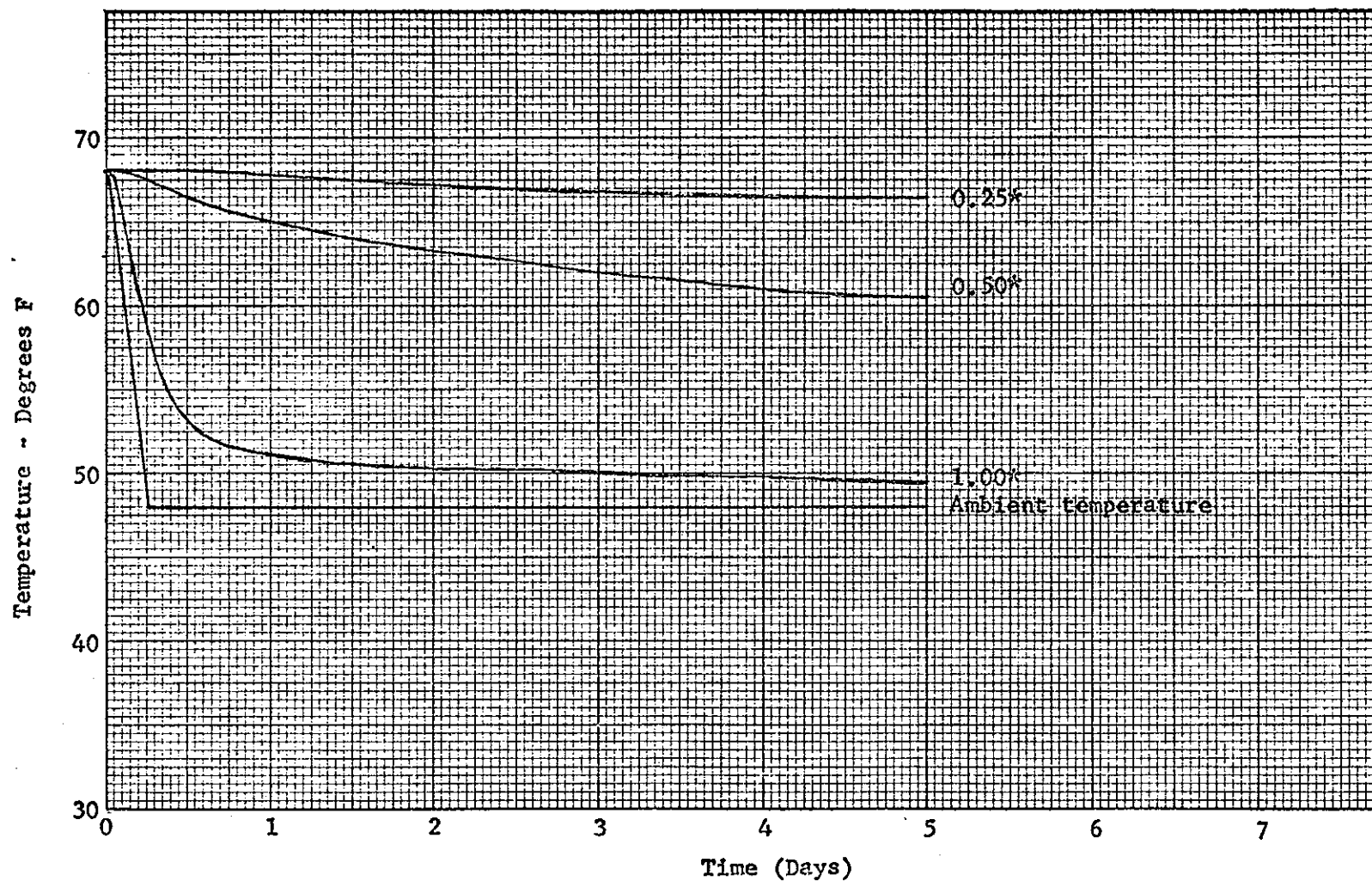


Fig. 30. Effect of Drop in Temperature on Surface Concrete with Insulation

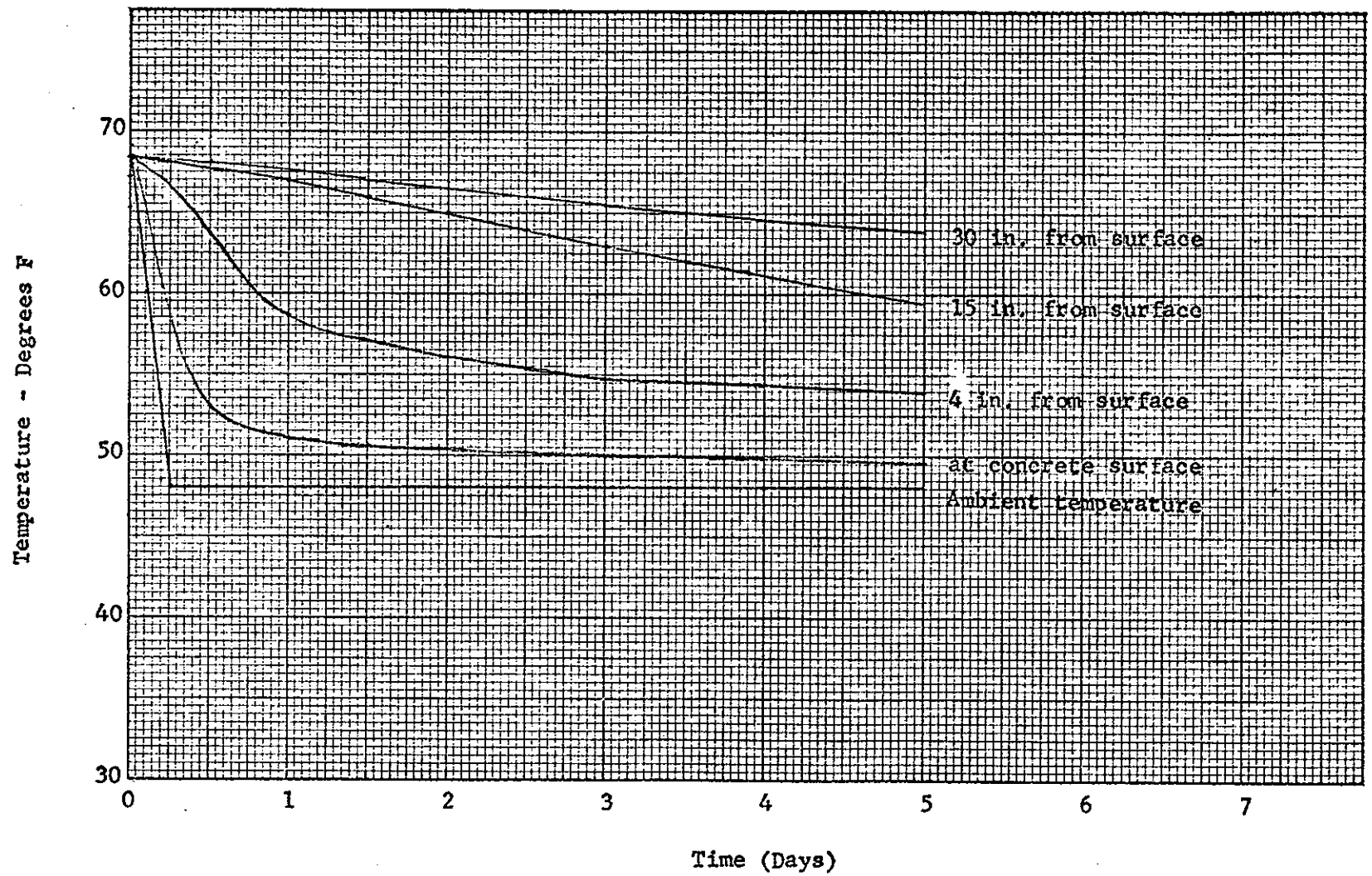


Fig. 31. Effect of Temperature Drop on Interior Concrete Near Exposed Surface (No Insulation)

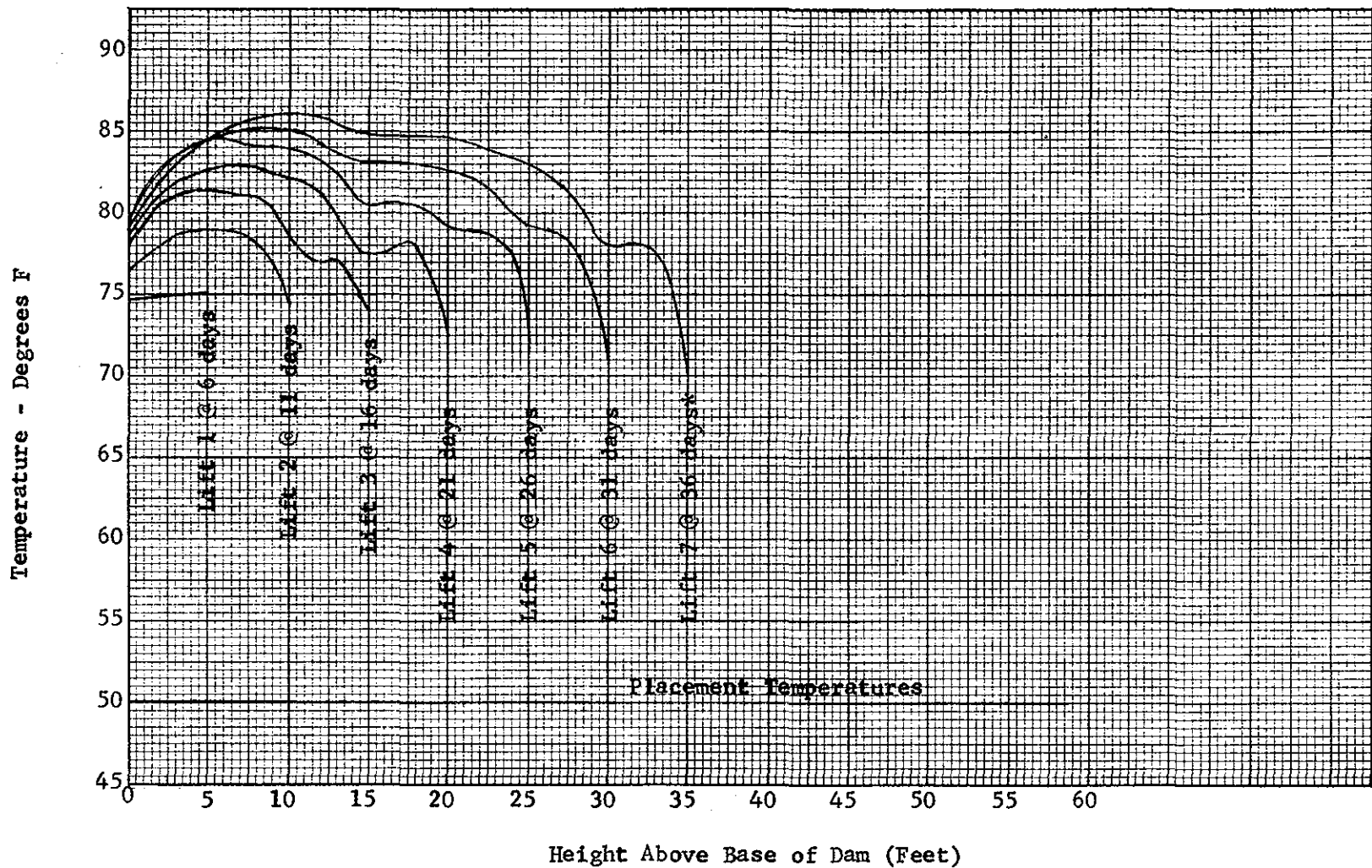


Fig. 32. Vertical Thermal Gradients Prior to Placement of Next Lift
Along Line ABCDEFG, Fig. 20

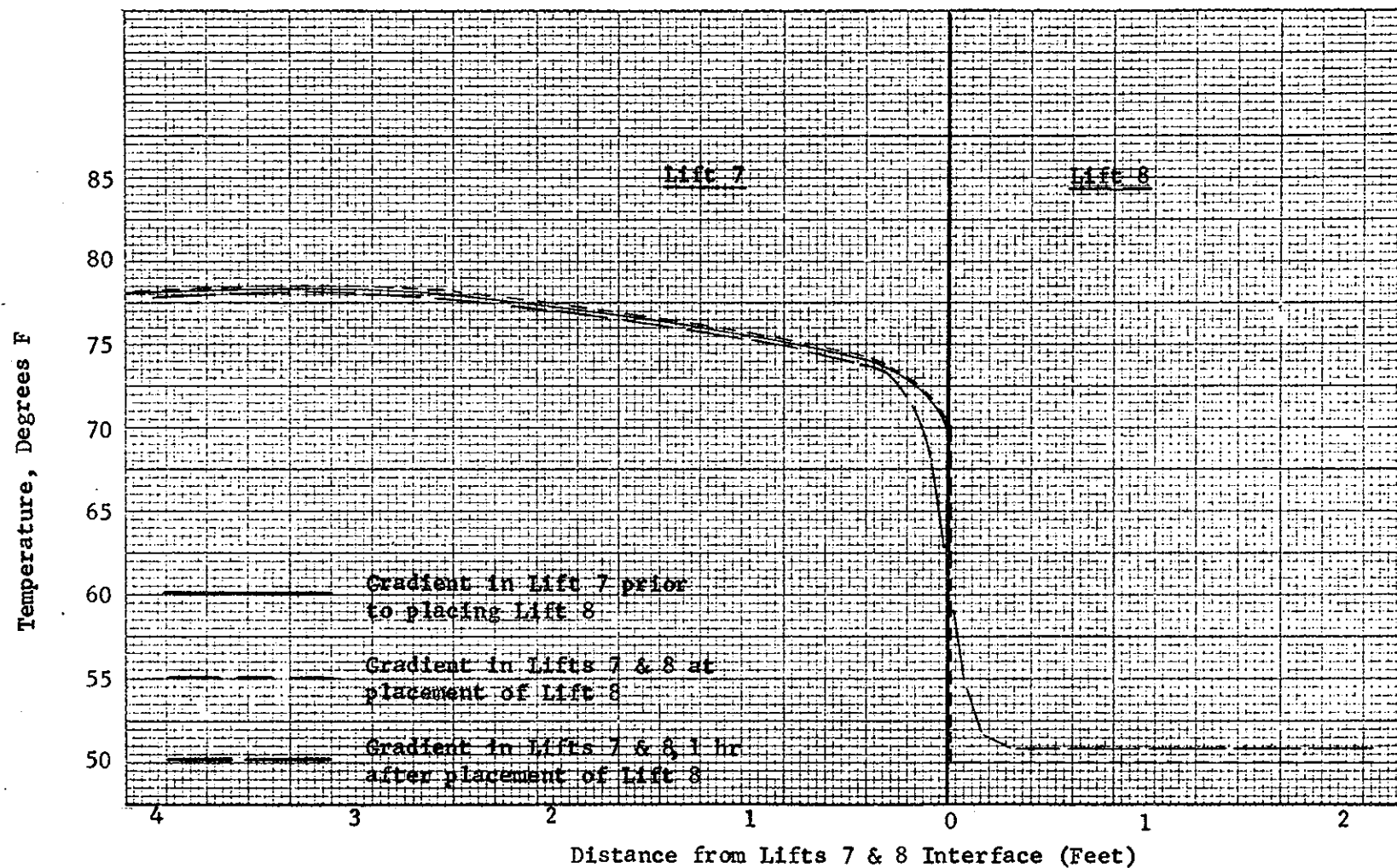


Fig. 33. Thermal Gradients Across Lift Interface

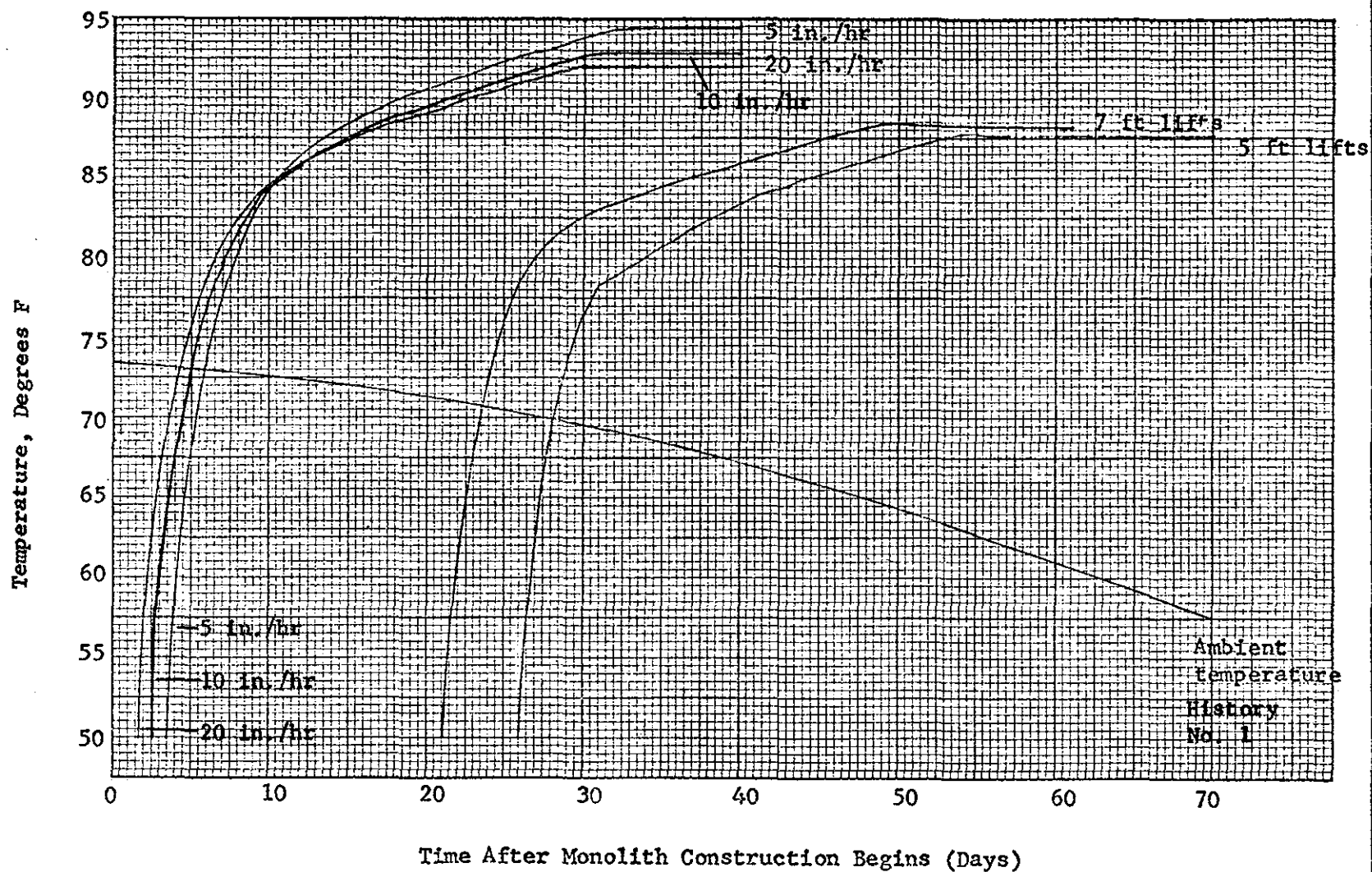


Fig. 34. Maximum Temperature Rise at Various Placement Rates

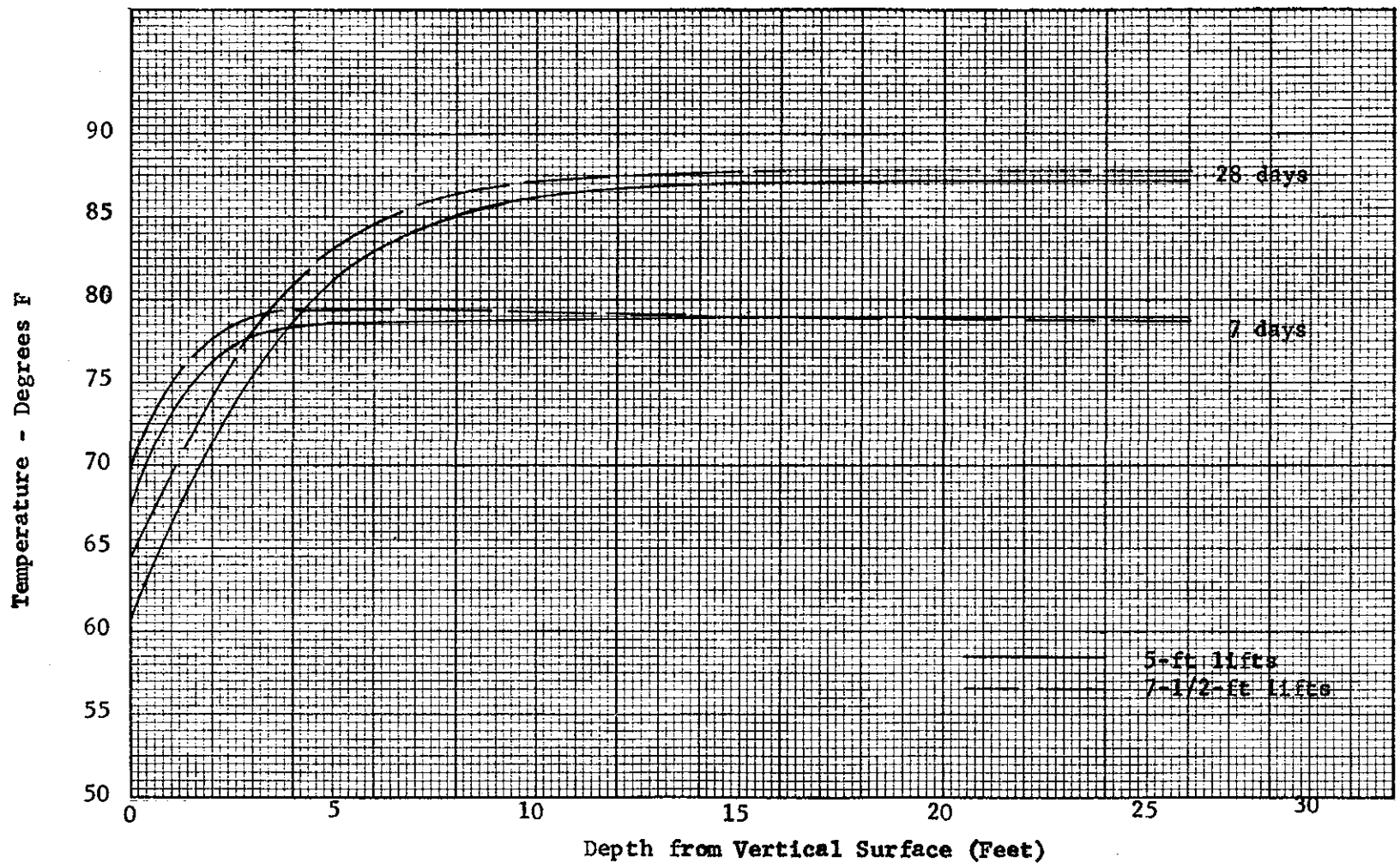


Fig. 35. Thermal Gradients - 7 and 28 Days After Placement

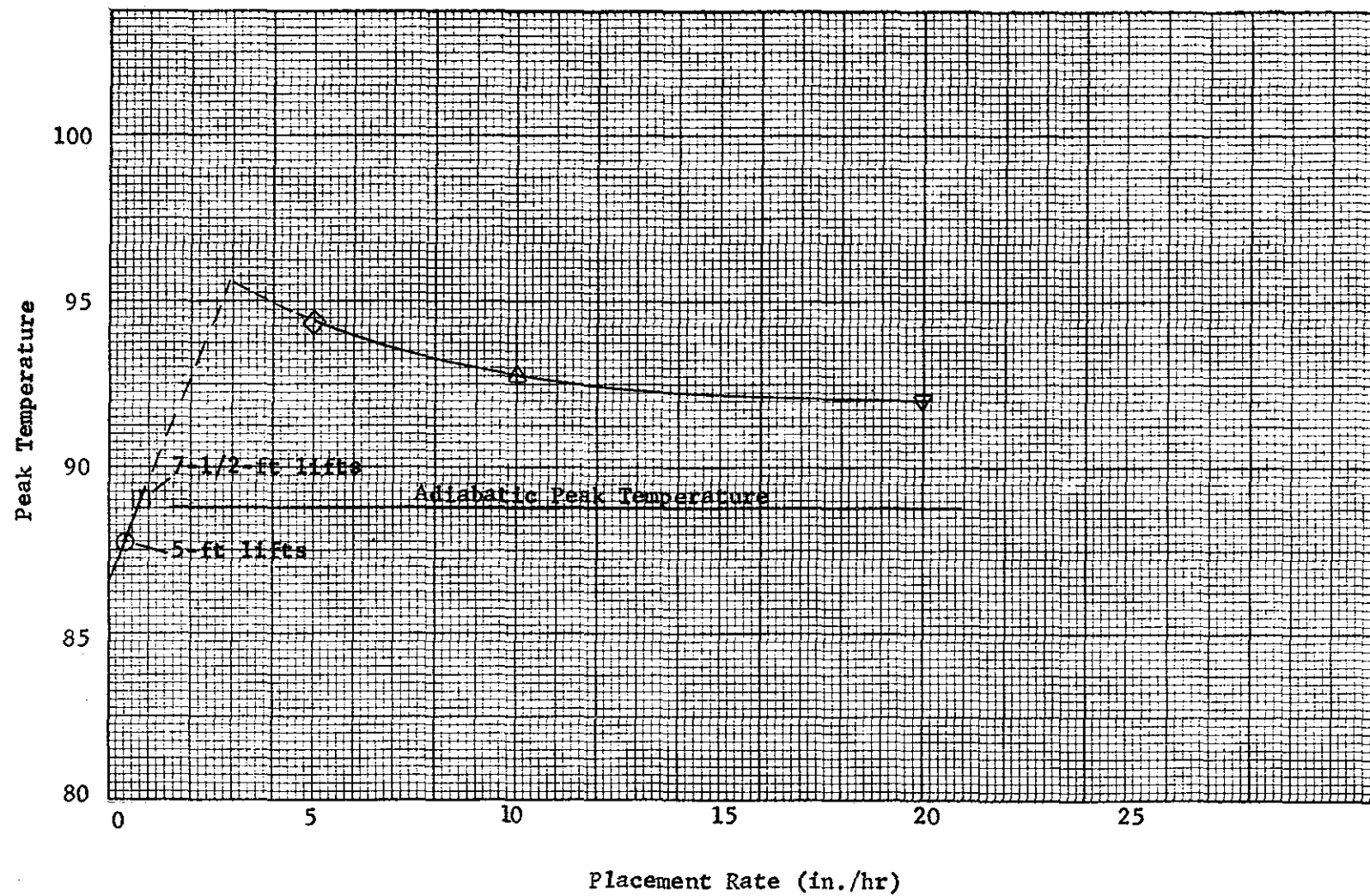


Fig. 36. Placement Rate Versus Peak Temperature

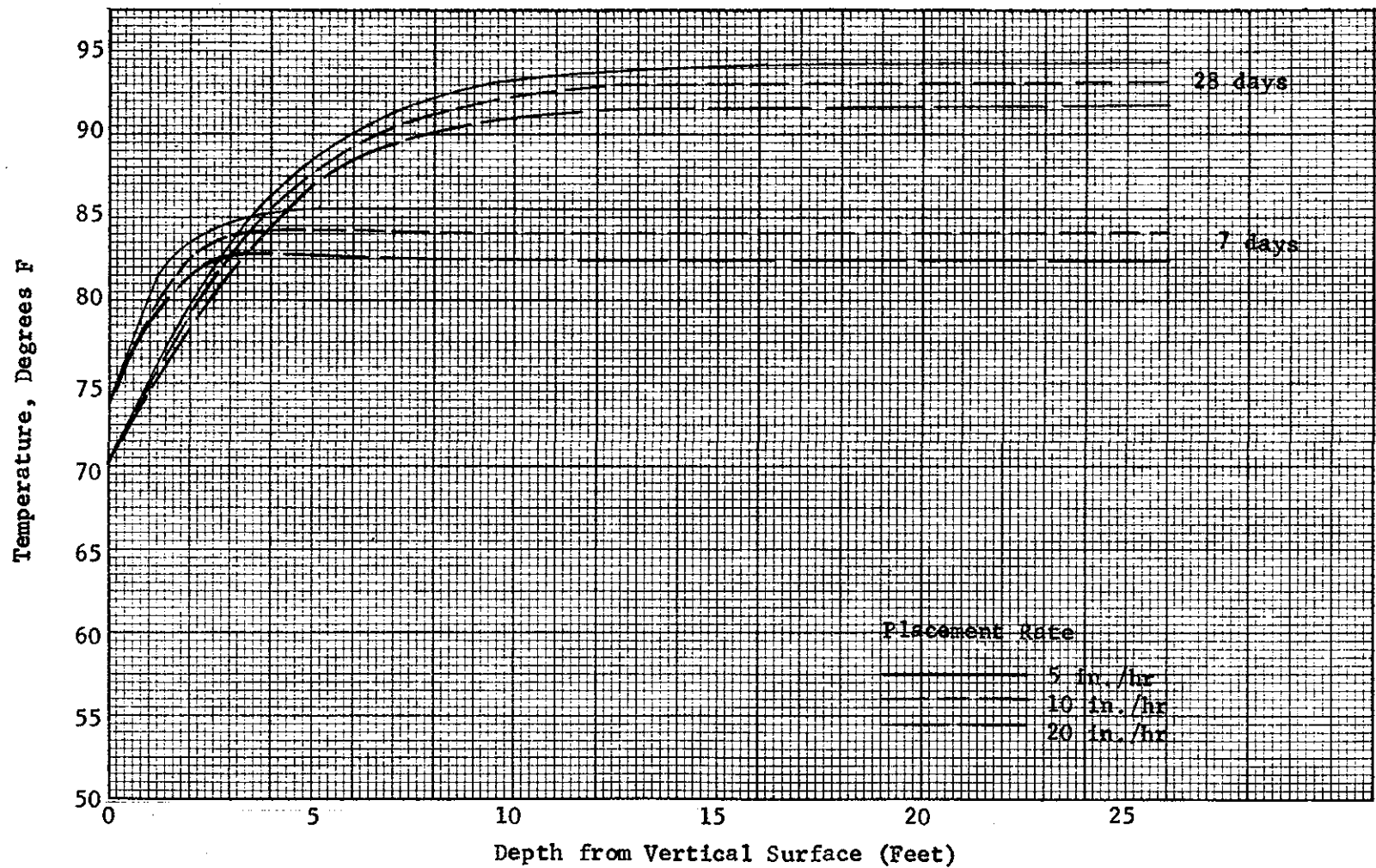


Fig. 37. Thermal Gradients - 7 and 28 Days After Placement

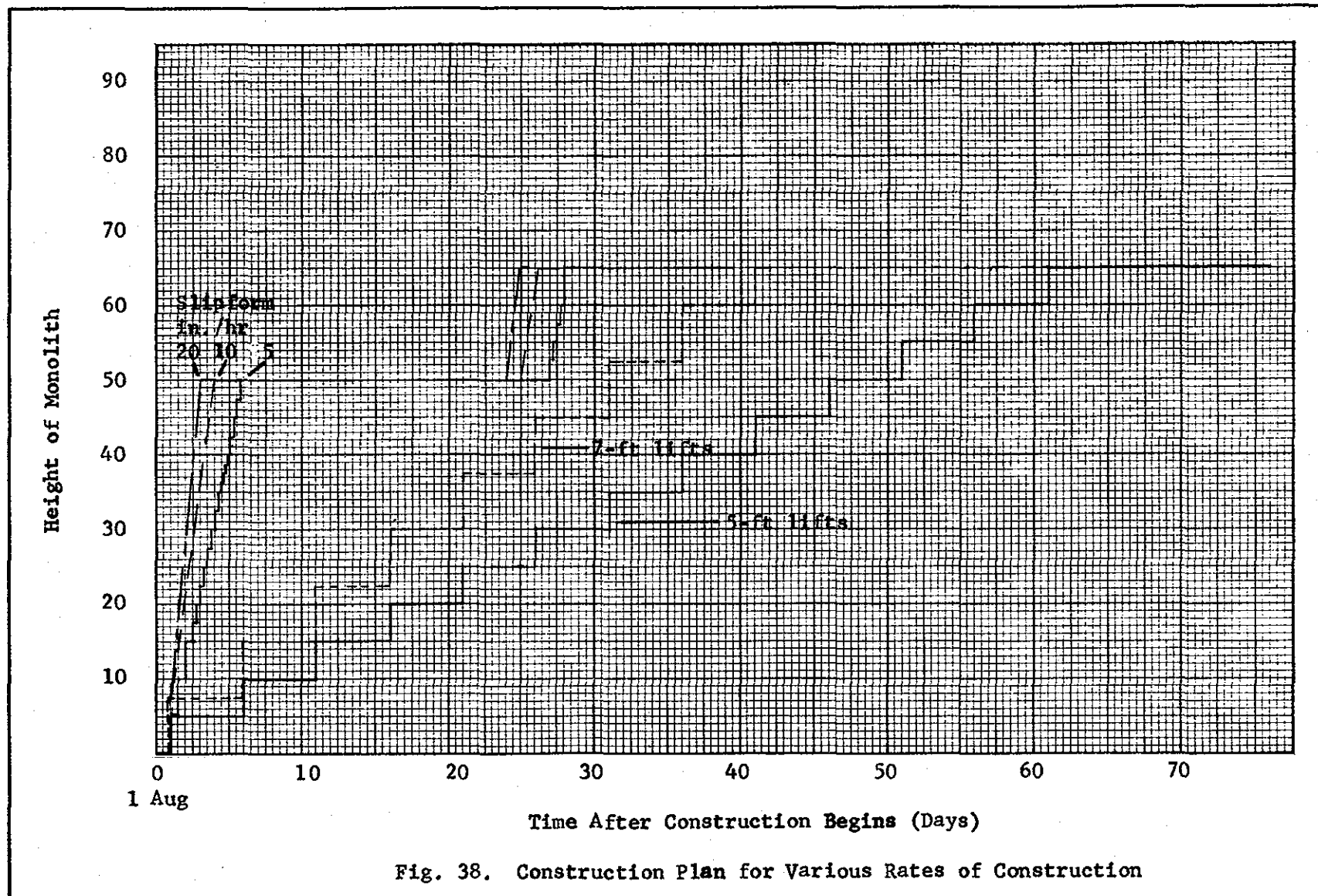


Fig. 38. Construction Plan for Various Rates of Construction

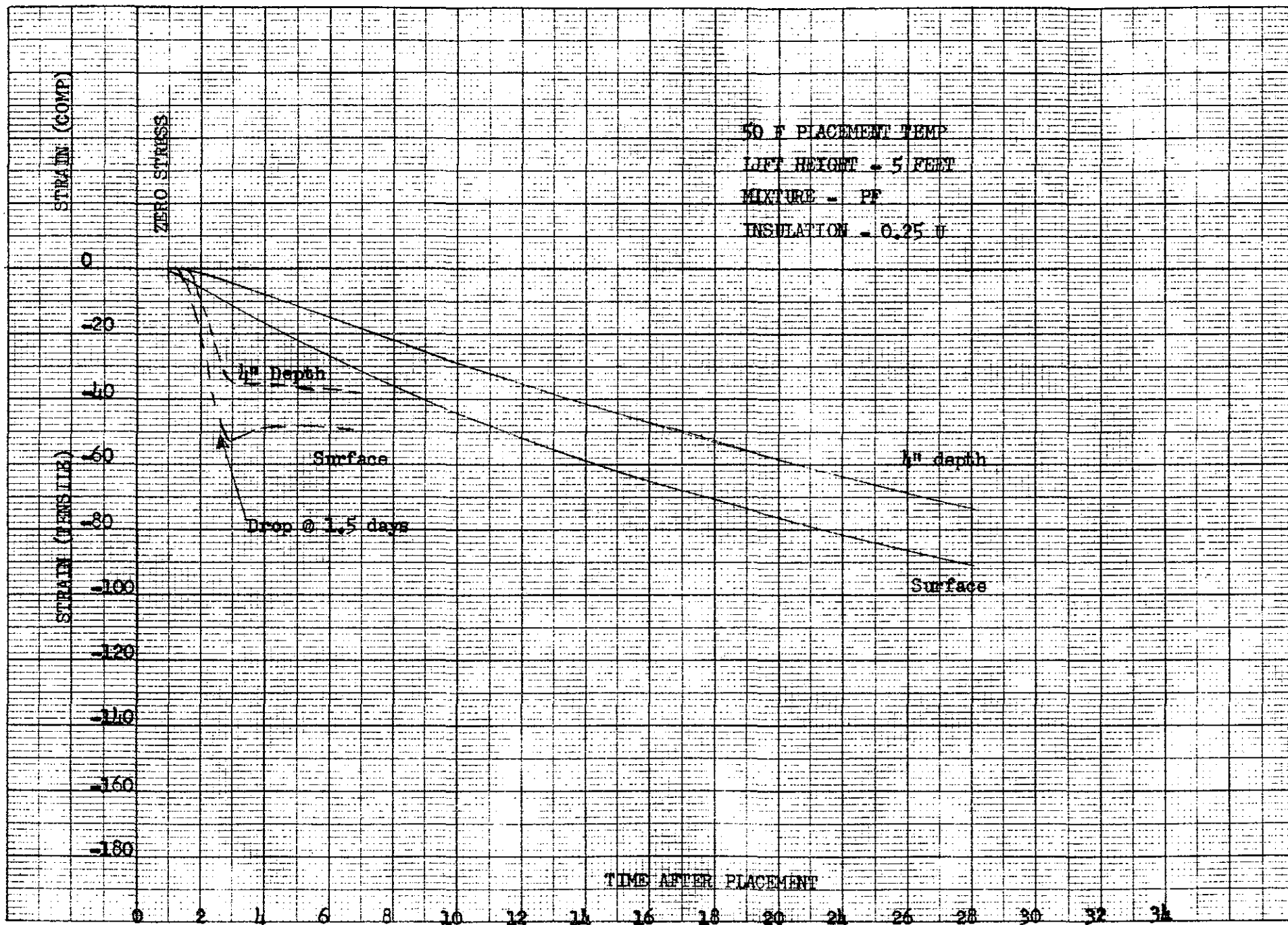


Fig. 39 Thermal Strains (Plot 1)

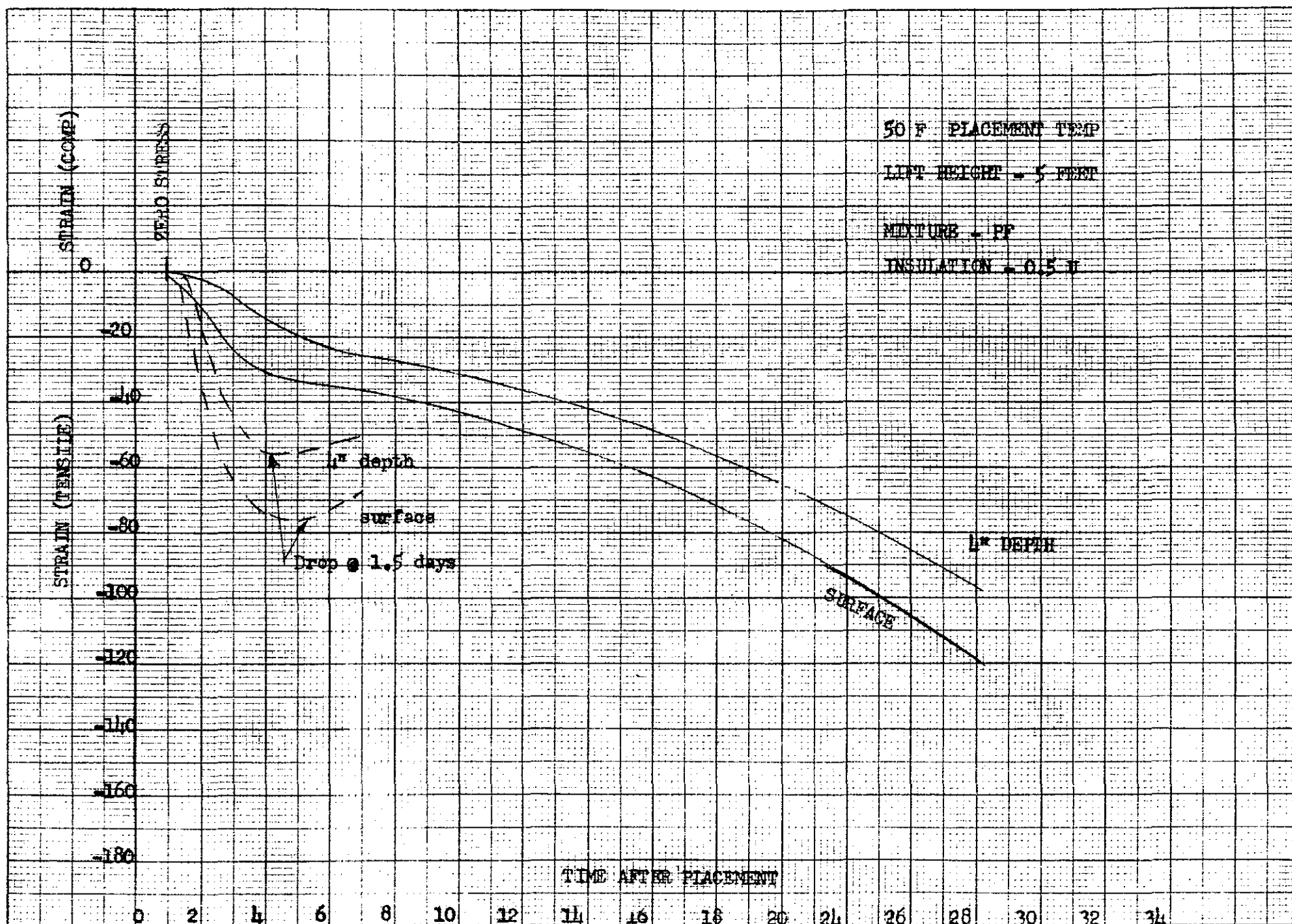


FIG. 1.C. THERMAL STRAINS (PLOT 2)

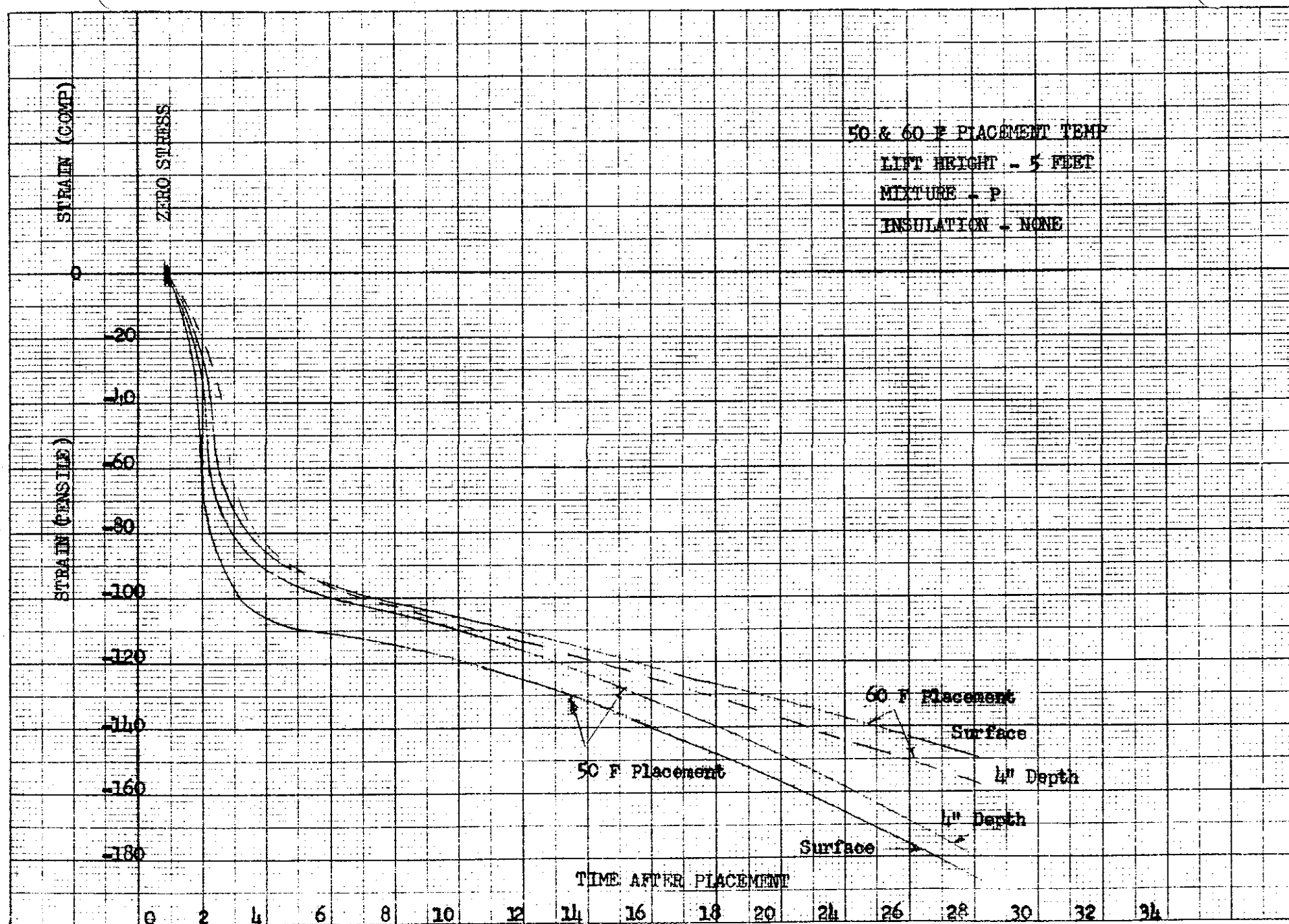


FIG. 41 THERMAL STRAINS (PLOT 3)

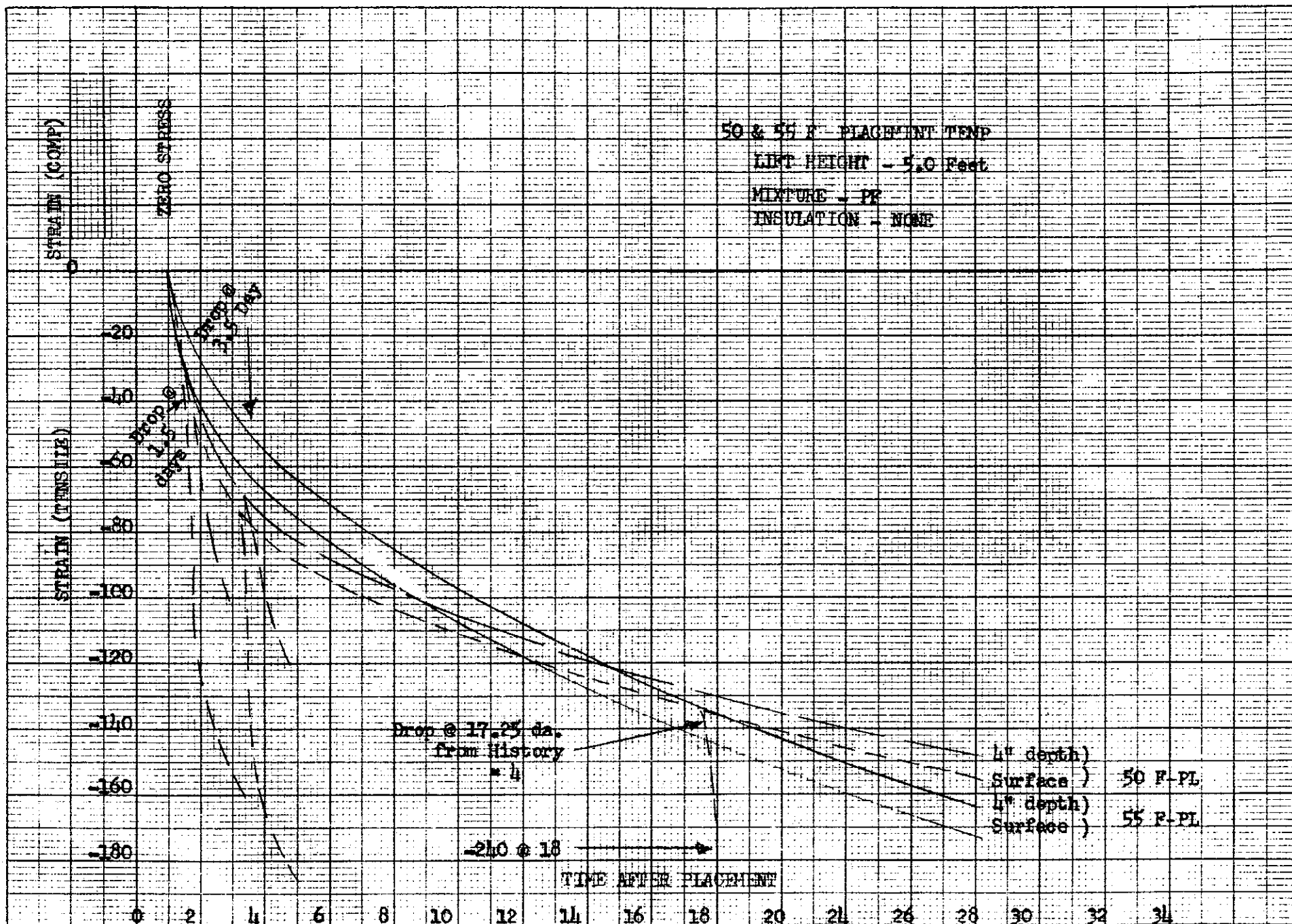


FIG. 42 THERMAL STRAINS (PLOT 4)

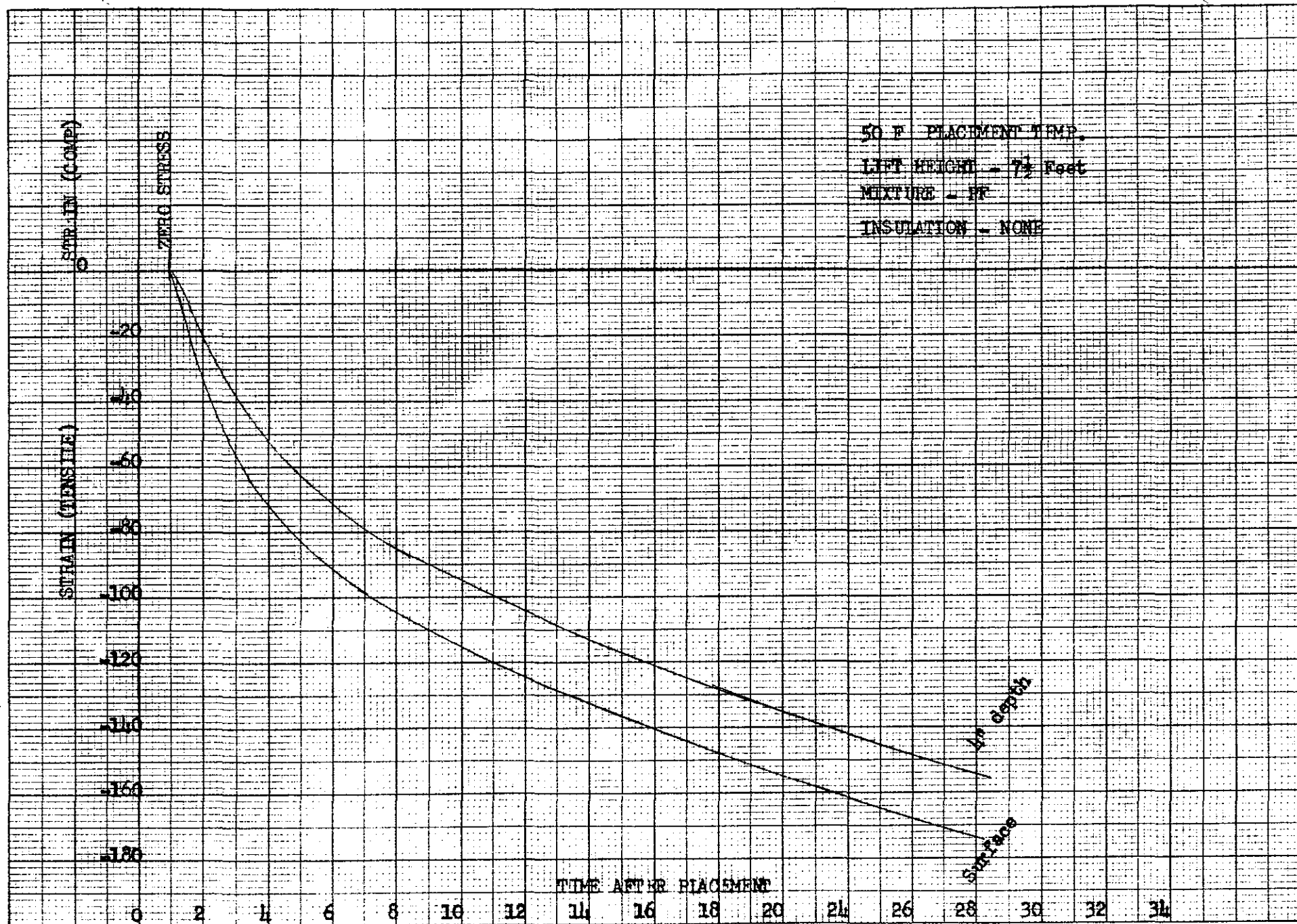


FIG. 43 THERMAL STRAINS (PLOT 5)

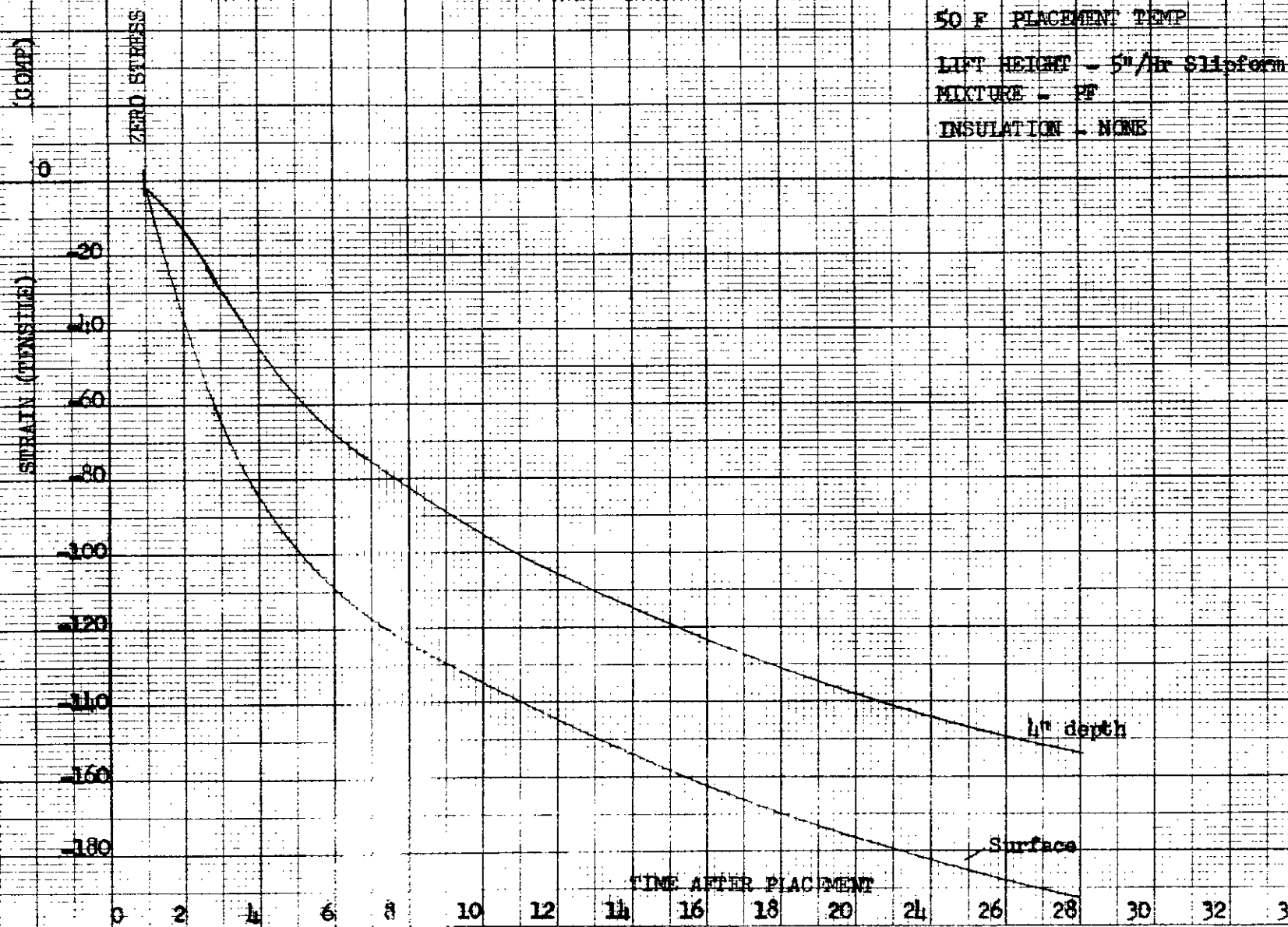


FIG. 15 TENSILE STRAINS (PLOT 6)

RUN NO.	LIFT TH. (FT.)	MIX NO.	INSULATION	PLACEMENT TEMP (°F)	TEMP @ ZERO STRESS (1-Day)	@ Elevation 7-1/2 Feet			FINAL TEMP @ CENTER	NET STRAIN CHANGE FROM MAX CENTER	NET STRAIN CHANGE CENTER	FINAL TEMP @ HEEL (°F)	NET STRAIN CHANGE from (ZERO STRESS) @ HEEL	RUN NO.
						MAX. TEMP. OF	AGE DAYS	STRAIN CHANGE (U°)						
1	5	PF	1.0	50	60.7	85.4	28	+139.9	50	-194.7	-54.8	40	-113.9	1
2	5	PF	1.0	55	65.7	87.9	28	+122.1	50	-208.5	-86.4	40	-141.4	2
3	5	PF	1.0	60	70.7	90.1	28	+106.7	50	-220.6	-113.9	40	-168.9	3
4	5	P	1.0	50	60.7	88.6	28	+167.4	50	-227.7	-60.3	40	-119.3	4
5	5	P	1.0	60	70.7	93.0	28	+133.8	50	-253.7	-119.9	40	-178.9	5
7	5	PF	0.50	50	60.7	86.8	28	+113.6	50	-202.4	-58.8	40	-113.9	7
8	5	PF	0.25	50	60.7	86.8	28	+113.6	50	-202.4	-58.8	40	-113.9	8
11	7 1/2	PF	1.0	50	60.7	86.6	28	+112.5	50	-202.4	-59.9	40	-113.9	11
12	5 1/2 AR	PF	1.0	50	64.5	91.9	28	+150.7	50	-230.5	-79.8	40	-134.8	12

FIG. 45 - TEMPERATURE CALCULATIONS